CHALMERS

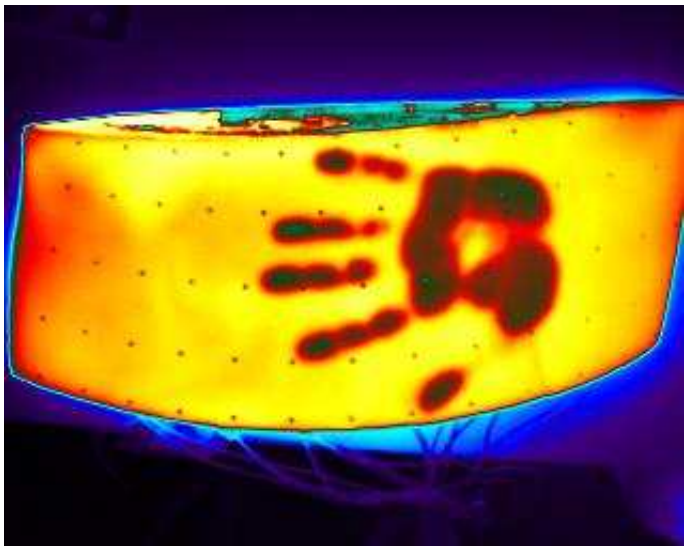

Experimental Heat Transfer Study in Intermediate Turbine Duct

Master's Thesis in Solid and Fluid Mechanics

Borja M. Rojo Perez

Department of Applied Mechanics
Division of Fluid Dynamics
Chalmers University of Technology
Göteborg Sweden, 2012

Master's Thesis [2012 : 41]

Master's Thesis 2012:41

Experimental Heat Transfer Study in Intermediate Turbine Duct

Master's Thesis

Borja M. Rojo Perez

Department of Applied Mechanics
Division of Fluid Dynamics
Chalmers University of Technology
Göteborg, Sweden, 2012

Experimental Heat Transfer Study in Intermediate Turbine Duct
Master's Thesis
Borja M. Rojo Perez

Master's Thesis 2012:41
ISSN: 1652-8557

Department of Applied Mechanics,
Division of Fluid Dynamics
Chalmers University of Technology
Se-412 96 Göteborg, Sweden
Phone +46-(0)31-7721400
Fax: +46-(0)31-180976

Printed at Chalmers Reproservice
Göteborg, Sweden 2012

Borja M. Rojo Perez
Master's Thesis
by
Borja M. Rojo Perez
mail@student.chalmers.se
Department of Applied Mechanics
Division of Fluid Dynamics
Chalmers University of Technology

Abstract

This master thesis report presents an experimental study of the heat transfer in an agressive intermediate turbine duct (ITD). The aim of this study is the visualization of a surface temperature distribution and convection heat transfer coefficient with a very high resolution and precision of vane which is located inside the ITD in order to understand the heat transfer mechanism in the intermediate duct.

The intermediate turbine ducts are used in modern jet engines to guide the flow from the high-pressure turbine (HPT) to the low-pressure turbine (LPT). This experiment was done in a state-of-art aggressive intermediate turbine duct in a large-scale low-speed turbine facility. The purpose of this design is to have a realistic inlet conditions and a Reynolds number. The measurements were performed by using the *Infrared Thermography*. In order to use this method, an infrared imaging camera is necessary and vane has to be specially prepared and instrumented.

The results of this experiment will be used for CFD validation and these results will help to understand the heat transfer mechanisms inside the ITD. First of all, I would like to express my gratitude to my supervisor Martin Johansson. His patience from the beginning when I did not know hardly anything about laboratory equipment and his support during all the time that I spent doing my paper were of invaluable help.

Acknowledgement

First of all, I would like to express my gratitude to my supervisor Martin Johansson. His patience from the beginning when I did not know hardly anything about laboratory equipment and his support during all the time that I spent doing my paper were of invaluable help.

I would also like to deeply thank to Professor Valery Chernoray for all his help and his availability whenever it was needed. His knowledge in all the areas concerning to this master's thesis project was a great help.

I wish to thank my coordinator in Spain Jorge Muoz for his advices and for his comments in order to improve the quality of this paper.

I also thank Maxim Golubev for his help manufacturing and for taking the images during the experiment. He makes much easier to work when the errors appear and he showed me that it is impossible to avoid them sometimes. I also thank Guglielmo Minelli and Amirreza Moghar for helping anytime I need their knowledge and for spending such a good time with them doing fika.

Furthermore, I thank to my family for all the support that they gave to me during all my time Sweden. Without them it would be impossible to achieve all my goals. Thanks to all my Erasmus friends that I met during this wonderful year, specially to Gloria, Martin and Julia. I probably spent my best time with them.

Last but not least I am deeply grateful to my friends Alberto San Francisco and Alberto Pionosa who have always made me feel happy even during the hardest moments.

Thanks to Mnica Marcos for teaching me the value of friendship no matter the circumstances.

Contents

Chapter 1

Introduction

Modern jet engines need more and more energy efficiency, less noise levels and the same or even higher power output. This requirements can be achieve by increasing the engine bypass ratio, which requires ITD with higher radial offset. At the same time, it is necessary to avoid heat transfer losses and flow separation due to an aggressive shape of this ITD. Then it is needed to include in the ITD guide vanes in order to avoid this losses. Making this experiment will help to predict this losses.

1.1 Main objective

The purpose of this Master's thesis project is to measure the convection heat transfer coefficient on the surface of a vane situated in the intermediate turbine duct (ITD). This information is very important to understand better the heat transfer mechanism inside the ITD and for CFD validation purposes. There are two ways to obtain this information, imposing a known temperature distribution along the surface or a known surface heat flux. With one of these conditions it is possible to obtain the convection heat transfer coefficient.

1.2 Measurement Methods

Logically, any heat transfer experiment needs to have a heat source. The heat source should be in the fluid (e.g., heating up the fluid with electrical resistors) or the solid by heating it up on its surface or inside the solid. The most suitable choice is to heat up the solid.

The solid can be heated up by heating foils on the surface. The heat flux could be directly measured knowing the electric power and dividing it by the

area of each electric foil. Using electric heating foil could be a good solution but due to geometrical issues (the vane is very three-dimensional) and that there would be an unknown small fraction of the heat flux that will go to the core of the vane instead of the air, even if the surface material has low conductivity.

Figure 1.1: Heating foil.

There is a surface treatment can be used for this kind of experiment. It is called thermochromic liquid crystal. This technique gives information of one surface (instead of one single point) and can be used for this experiment. The vane would be covered with a thin film (liquid crystals) which reflects specific wavelength in visible spectrum dependent on the temperature. Furthermore, a digital color camera and white light are necessary to use this technique. The main problems of this technique are the deterioration of the liquid crystals with the time and the color (wavelength) dependence with the angle.

Another technique to obtain the heat transfer coefficient along the vane is the measurement of a finite number of temperatures on the surface using thermocouples or resistance temperature detectors. The difference between them is that the thermocouples give an electrical signal (voltage) which is dependent on temperature and the resistance temperature detectors change the electrical resistance with the temperature and it can be measured by an ohmmeter. The main advantages of this method are the accurate results (0.1-0.01C precision for thermocouple and 0.01C for thermoresistance) and the simplicity of this method. The disadvantage is the difficulty of manufacture a vane with a big amount of these instruments in order to have a complete map of temperatures and consequently the convection heat transfer coefficient distribution.

Finally, the technique that is used for this experiment is based on imaging by an IR-camera (Infrared thermography). It is required to have a surface painted with special black coating with very high emissivity and very low angle dependence. With this method it is possible to obtain a high spatial

resolution of the temperature on the vane surface if the optical access is provided. The vane is a solid that is heated up with electrical resistance heaters and has an elevated temperature up to 60 degrees along the core. Then covering this core with a shell made of an isolated material strong temperature gradient is created and with the IR-camera it is possible to measure the temperature and evaluate the heat flux and convection heat transfer coefficient.

Figure 1.2: Camera pointing at the vane during experiment.

1.3 The Vane

The design of the vane geometry is done by Volvo Aero Corporation. The hardware implementation design for the rig is performed at Chalmers. During the project the vane material design has been changed because different problems that will be explained. The original design is basically a solid machined aluminium vane covered with a 5 millimeters constant thickness layer of epoxy resin. The core of the vane has 8 holes where the electrical heaters can be inserted. The weight of the vane is approximately 12kg and it is important to notice that if the core of the vane was made of another material like copper, the weight could be more than three times higher.

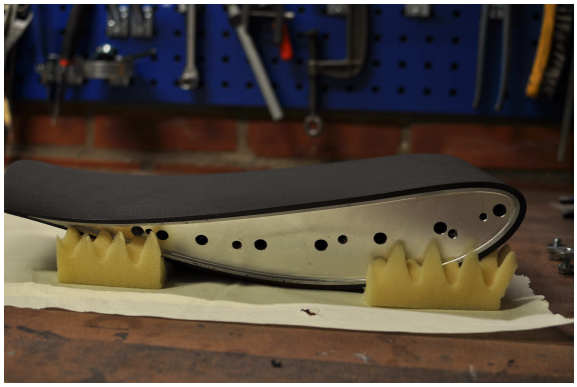

Figure 1.3: Epoxy vane after painted with coating

The purpose of this composite piece is to perform a heat transfer experiment. The reason for using aluminium core and epoxy resin shell is the difference of conductivity of these materials (epoxy's thermal conductivity is 1000 times compared to aluminium). The aluminium has the maximum thermal conductivity as possible in order to have a constant temperature in the core (see Setup of Heat Transfer Measurement). The figure below shows how this principle works in the simple case of 1D thermal conduction.

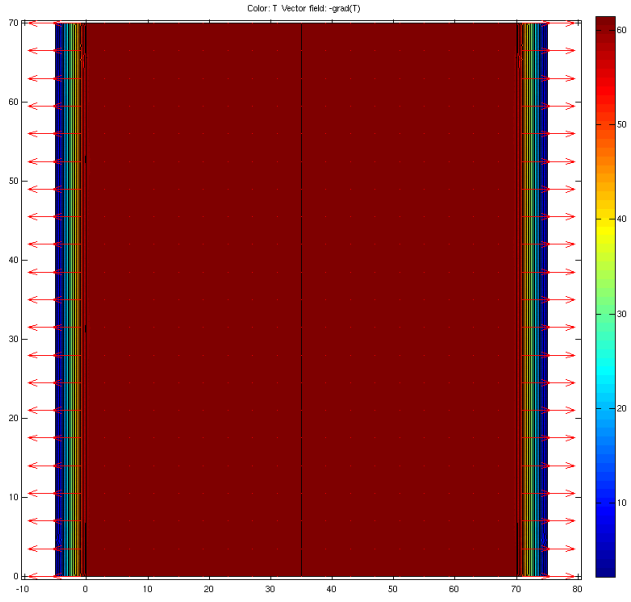

Figure 1.4: 1D case using PDETOOL in MATLAB

In the figure above, up and down edge boundary conditions are Neumann homogeneous. Right and left edge boundary conditions are Neumann non

homogeneous (convection heat flux with h=50 W/m^2.K is equal to conduction heat flux). Aluminium core (middle) has an homogeneous heat source. It can be seen in the Fig.1.4 that the aluminium core has a very homogeneous temperature distribution, almost constant temperature. A suitable assumption to have an approximately idea about the heat flux after the experiment could be that the temperature distribution in the epoxy layer is linear, which is almost a realistic case.

It was critical to avoid bubbles inside the vane due to the fact the air has very low conductivity (10 times lower than epoxy resin). Unfortunately, this first vane design did not work because it was broken due to forces that appear during the polymerization process and cooling cycle after doing a thermal test of the vane at 60 degrees. During the polymerization the epoxy shrinks by approximately 1%. During the thermal cycle the epoxy can be deformed up to a 0.2% and the aluminium only 0.1%. This fact produces two negative effects. The first one is that appear the forces that I mention before and the second one is that due to the pressure side has a negative curvature and the materials have different deformation, the epoxy resin is detached from the vane. In Fig. 1.5 is shown the consequences of these effects.

a) 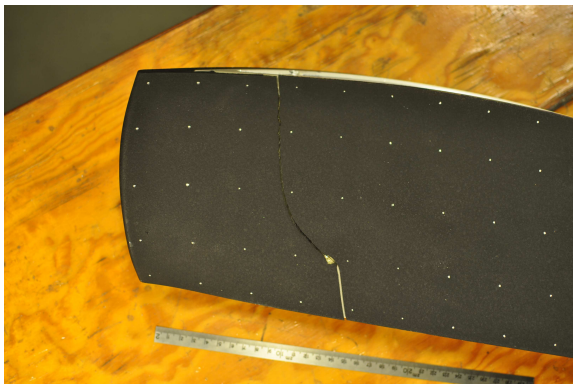 b) 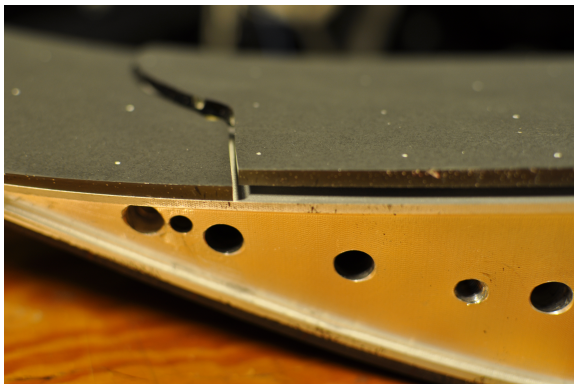

Figure 1.5: Pictures of the broken vane with epoxy shell

After, the second vane design the aluminium core with heating foils on the surface painted with the black paint. This idea had several problems. The main one was that it was impossible to have a uniform heat flux and temperature distribution under the separation layer of black tape which it was known its thickness and its emissivity and it was impossible to know which part of the heat flux goes to the vane an which one goes to the air. Another very important problem was the difficulty of gluing these heating foils without any bubbles.

Then, another design of the vane was consider. The idea is almost the

same as the previous design, but instead of heating foils there were *kapton* foils. This material has a low conductivity (one of its application is for thermal isolation in space shuttles) and can generate a very big gradient if there is a heat source inside the aluminium core. The problem of this material is that it was very thin and it was very sensible to have bubbles. Also the vane is three-dimensional to be able to cover the entire vane with this material.

Therefore, the vane design was changed by using the plastic vane model with the heaters inside. The way to obtain the heat flux would be measuring the temperature distribution over the surface of the vane and the heat flux of the heaters. Therefore, knowing these data and assuming that the sides of the vane are adiabatic, it would be possible to calculate the heat flux numerically. The problem of this vane was that the vane was broken after a thermal test.

Figure 1.6: Plastic vane

Finally, the last design and the one which was used in the experiment is a vane composed of an aluminium core and a 5 mm thick silicone shell. It was manufactured by me and Maxim Golubev. The core was the original aluminium core from the first vane and silicone was glued with special glue for silicone. The process to manufacture the vane shell was to make the

shell with 4 pieces of silicone. Spreading the glue with a uniform tension distribution, the vane shell was manufactured without bubbles. In Fig. 1.8 can be seen the process and the tools used for manufacturing this vane.

It is important to point out the silicone should be transparent instead of opaque because this is the best way to inspect if there are air bubbles. In case there are some bubbles left it is possible to remove them using syringe with some glue and solver inside. After manufacturing the vane, it was painted with black coating paint.

a) 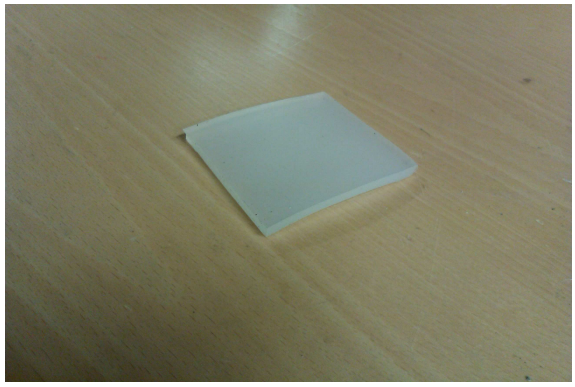 b) 

Figure 1.7: Silicone used for the vane shell

1)  2) 

3)  4) 

5)  6) 

Figure 1.8: Manufacturing process of the vane silicone shell.

Chapter 2

Theoretical Background

This chapter describes the theory behind the experiment. It also can help to understand all the assumptions that are behind of the experiment design. As this is mainly a Master's Thesis Project which study the heat transfer along a vane, the theory that is important to understand is based on heat transfer mechanisms.

2.1 Conduction

First of all, it is important to understand the three heat transfer mechanism that are involve in this project.

Conduction is a phenomenon that appears in solids. This can be explained as the transfer of energy from the more energetic particles (higher temperature) to the less energetic particles. Because of this, in any solid which has any temperature difference (gradient) this heat transfer mechanism will appear. For the calculation of the heat flux it Fourier's law is used which is:

$$q'' = -k\nabla T[4] \tag{2.1}$$

This formula will be used during the post-procesing calculation in order to calculate the heat flux over the surface of the vane.

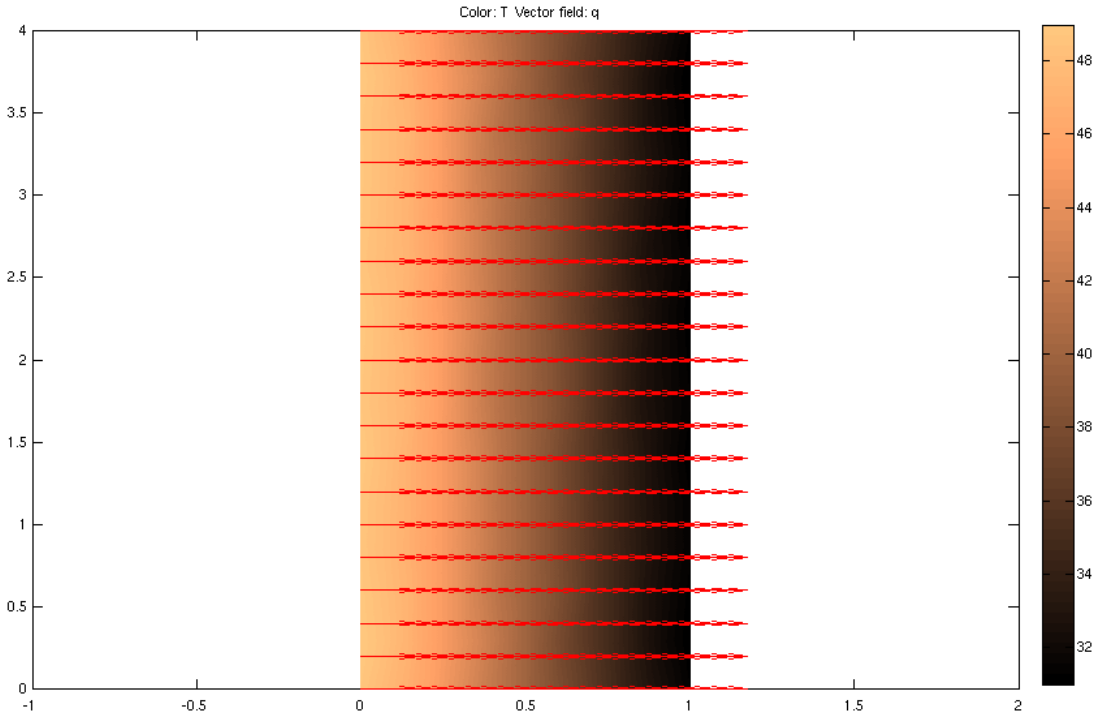

Figure 2.1: Condunction example using PDETOOL in MATLAB

It is also very important to take into account that the aluminium of the core let us assume that the temperature in each point of the core is approximately the same. This assumption will be checked during the experiment and using CFD simulations.

2.2 Convection

Convection is a phenomenon that appears in heat transfer between liquid-liquid, gas-liquid, gas-gas, solid-liquid and solid-gas. It is much more complex to study convection than conduction due to the fact that it is dependent on much more variables than conduction. In this case, the convection will appear between the silicone outershell of the vane and the air at room temperature.

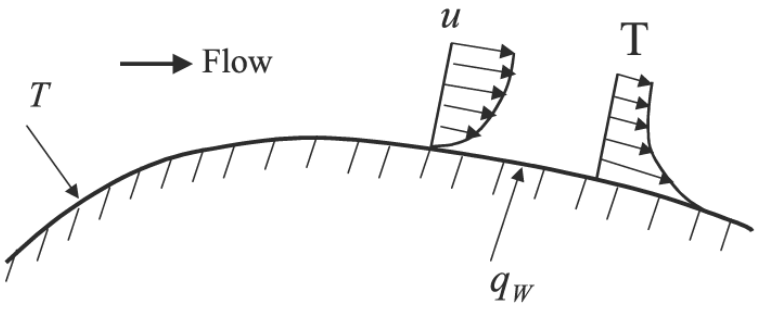

Figure 2.2: Convection example for solid-liquid. Temperature boundary layer [6]

As it can be seen in the figure above, there is a temperature distribution dependent on the position. In order to calculate the heat flux between the solid wall and the fluid *Newtonś law* is used.

$$q'' = h(T_{wall} - T_{\inf})[4] \tag{2.2}$$

It is important to point out three factors. First one is that T_{inf} is the temperature of the fluid far enough from the wall. Second factor is that the convection heat transfer coefficient h dependant on the fluid flow, so it is difficult to calculate this value. The last factor to point out is that this heat transfer mechanism only depends on the surface temperature, and then the temperature distribution inside the solid is something that can be ignored when calculations of heat transfer by convection are made.

The aim for this project is to calculate h (W/m^2.K) along the vane.

2.3 Radiation

The existence of vacuum between two bodies implies that there is no thermal conduction and convection heat transfer, because in both cases is needed matter. So the question is for example, how can the sun heat up the planet Earth if there is no matter in between. The solution for this question is another heat transfer mechanism, *radiation*. Then, if two bodies have different temperature in an isolated system, even with nothing else between them, they will have the same temperature in the long term just because of this principle.

Hence, all bodies transmit energy by radiation. The bodies emit electromagnetic radiation in a range of wave length dependent on their temperature. This temperature dependence is as the convection case, only depends on the surface temperature. Due to the fact that thermal radiation is transferred by

electromagnetic waves, it means that temperature is related with frequency and wave length. The first and simplest case that was explained using this theory is the radiation by a blackbody. This case is explained by *Planck's law.*

$$I_{\lambda,b}(\lambda,T) = \frac{2hc_0^2}{\lambda^5(e^{\frac{hc_0}{k\lambda T}}-1)}[4] \tag{2.3}$$

Where $I_{\lambda,b}(\lambda$,T) is the spectral intensity and $h = 6.626\text{x}10^{-34}$ J.s and $k = 1.381\text{x}10^{-23}$ J/K. This h is known as *Planck's constant* and k is known as *Boltzmann's constant* and c_0 is the speed of light. It is important to point out that the temperature has to be always in Kelvin in any radiation formula (in conduction and either in convection Celsius or Kelvin). Taken into account that a blackbody is a diffuse emitter (uniform radiation in all directions) the *spectral emissive power* is:

$$E_{\lambda,b}(\lambda,T) = \pi I_{\lambda,b}(\lambda,T) = \frac{C_1}{\lambda^5(e^{\frac{hc_0}{k\lambda T}}-1)}[4] \tag{2.4}$$

Equation 2.4 is known as *Planck's distribution.* Plotting this distribution for different temperatures the dependence between the wavelength and the maximum radiation intensity for each temperature can be visualized.

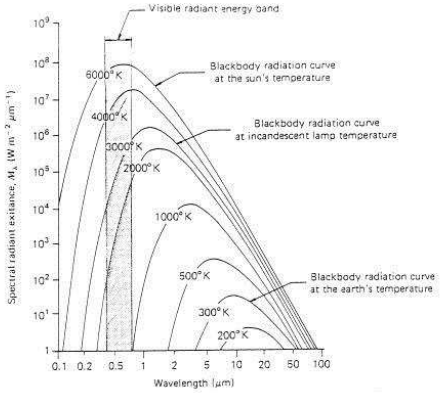

Figure 2.3: Spectral blackbody emissive power distributions

The wavelength and the maximum radiation intensity have a linear dependence. This relation can be obtained by differentiating the Eq.2.3 with respect to λ.

$$\lambda_{max} = \frac{C}{T} = \frac{2898}{T}[4] \tag{2.5}$$

Then, the emissive power is defined as:

$$E_b(T) = \int_0^{\infty} \int_0^{2\pi} \int_0^{\pi/2} I_{\lambda,b}(\lambda, \theta, \phi, T) cos\theta sin\theta \, d\theta d\phi d\lambda \int_0^{\infty} E_\lambda(\lambda) \, d\lambda [5] \tag{2.6}$$

In this case, it is assumed that the radiation is diffuse. Equation 2.6 can be used for calculating the emissive power even if the body is not *black* (emissivity dependant on the wavelength and not equal to 1). One simplification of this equation is the case of the *blackbody* which emissivity is equal to 1. The equation bellow shows this simplification.

$$E_b(T) = \sigma T^4 [5] \tag{2.7}$$

Where σ is the Stefan-Boltzmann constant ($5.669 \cdot 10^{-8}$ W/ $m^2 K^{-4}$).

Taking into account that the surface of the vane is painted with a special black coating which has diffuse radiation up to 60℃ and constant emissivity of 0.973, the radiation detected by the IR-camera is:

$$E_b(T) = \epsilon \sigma T^4 [4] \tag{2.8}$$

Chapter 3

The Experimental Facility

The main purpose of this project is to measure of heat flux along the vane. In order to run the experiment, an experimental rig which was built to study the intermediate turbine ducts was used. This chapter describes briefly the main characteristics, devices and instrumentation for running the facility.

3.1 General Characteristics

First of all, the main advantages of this rig can be summarized as follows.

At first is the possibility of having quantitative results instead of qualitative results. This rig experiments are advantageous to earlier experiments in this field which were done in facilities which lacked the main source of the inlet boundary conditions: the upstream turbine[1]. The difference between having a inlet with and without turbine is the *tip leakage flow* in the duct.

The second one is the flow quality and the repeatability of these experiment because the inlet flow should be as steady as possible in order to obtain reliable experiment results. In Fig.3.1 and the Table 3.1 there is a schematic of the facility and description of the facility characteristics.

[1] [1]

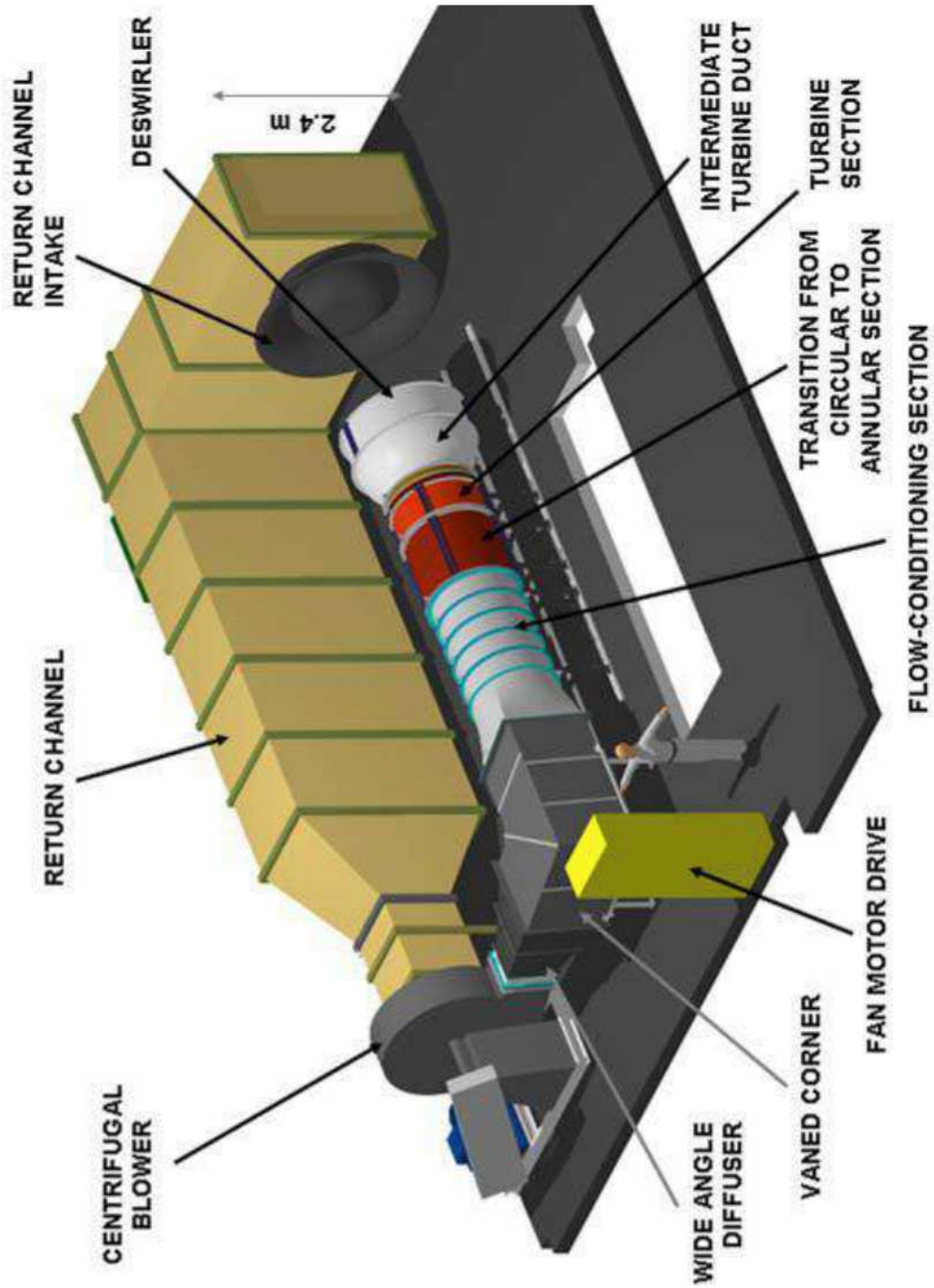

Figure 3.1: Experimental facility.[6]

Power of driving motor			110.0 kW
Design mass flow rate			10.0 kg/s
Pressure difference through blower at the design flow rate			6.6 kPa
Design turbine speed			1060.0 rpm
Maximum turbine pressure ratio			1.06
Brake	Maximum turbine speed		1300 rpm
	Maximum braking torque		400 kN.m
Design swirl angle from HPT			-17.5º
Duct geometry	Inlet	shroud radius	550.0 mm
		hub radius	440.0 mm
	Outlet	shroud radius	760.0 mm
		hub radius	635.0 mm
	Area ratio		1.6

Table 3.1: Most important characteristics of the facility.[1]

3.2 Turbine

The most special part of this facility is the turbine, which lets obtain a realistic inlet flow in the intermediate turbine duct (ITD). It simulates the flow through a high pressure turbine (HPT) in terms of flow conditions.

In this case, the HPT of the facility can rotate at a maximum speed of 1060 rpm (see in Table 1). A real HPT of a gas turbine engine rotates at a much higher speed than this one, but the flow Reynolds number and the outlet flow angle are the same (unity Reynolds number around $1.4 \cdot 10^6$ and Reynolds number based on axial chord 70000).

Therefore, these factors make possible to have realistic inlet conditions due to the tip leakage flow and correctly modeled incoming transient wakes. The diameters of the hub and shroud are 0.88m and 1.1m respectively. Fig.3.2 shows the turbine section that is described.

The HPT was designed by Rolls-Royce Deutschland. Turbine blades are made of polyurethane resin. Table 3.2 shows briefly the main design parameters of the HPT[2].

[2]It is important to point out that the number of stator vanes and rotor blades is 36 and 72 for a special reason. The ratio between them is an integer number, which helps CFD to decrease the computational time during the calculations

Geometry	Hub radius	440 mm
	Shroud radius	550 mm
	Blade tip clearance	1.6%
	Number of NGV's	36
	Number of blades	72
Operating point	Velocity ratio, Va/U (φ)	0,478
	Stage loading, $\Delta H/U^2$ (Ψ)	1,25
	Reaction	0,4986
	CpΔT/T	10467
	N/T^0.5	0.9309

Table 3.2: Most important characteristics of the HPT.[1]

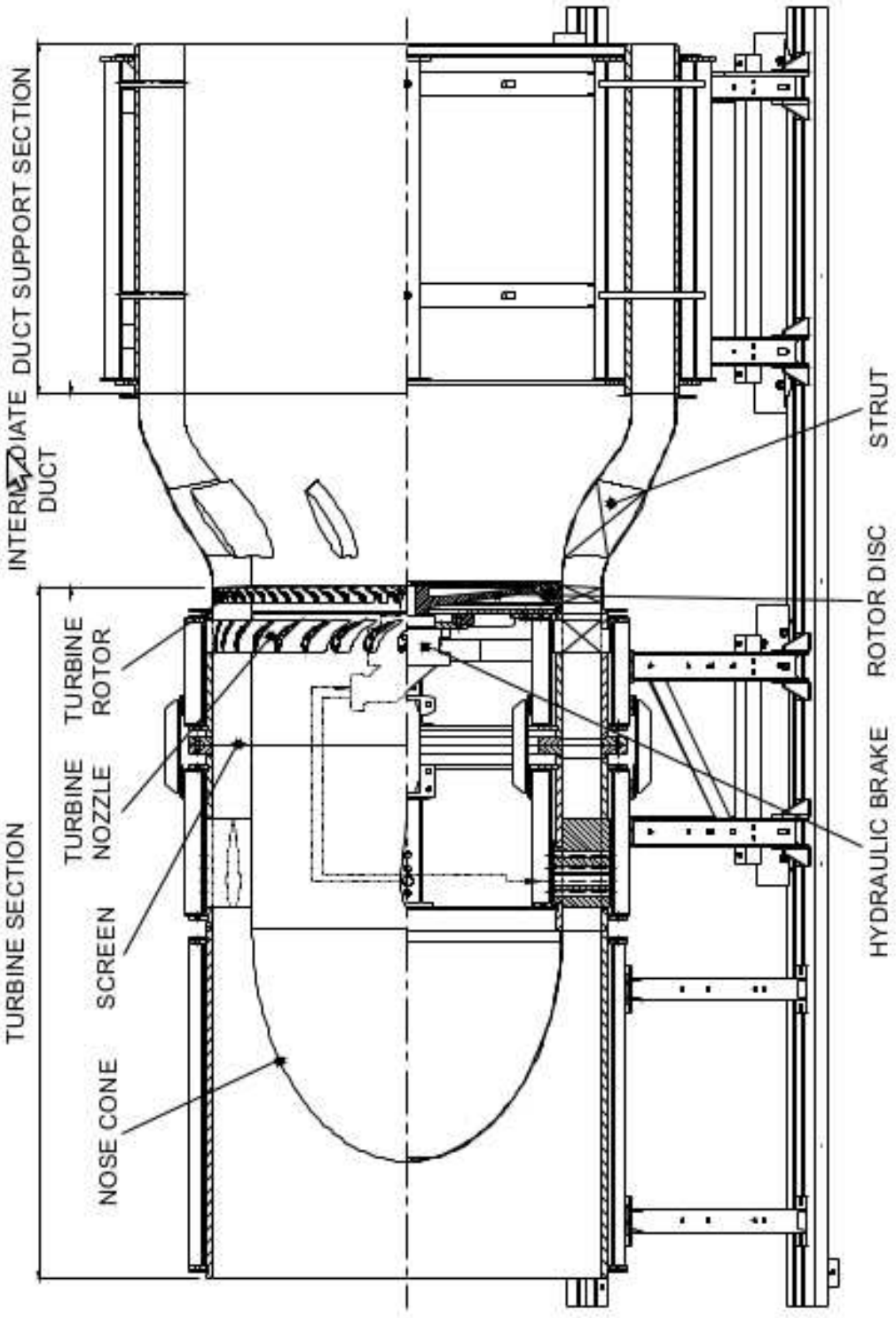

Figure 3.2: Turbine section.[1]

Furthermore, it is very important to install a brake system for the turbine for safety and controlling the operating point. In order to achieve steady conditions it is necessary that the control system is also very stable. Then, a hydraulic brake is used in spite of an electrical generator. This hydraulic brake uses oil as brake liquid and an oil/water heat exchanger (plate heat exchanger). The disadvantage of having an hydraulic brake instead of a electric generator is the torque control which is less accurate in the case of oil brakes. But hydraulic system is much less expensive and more compact. The hydraulic circuit is shown in Fig. 3.3 b).

a)

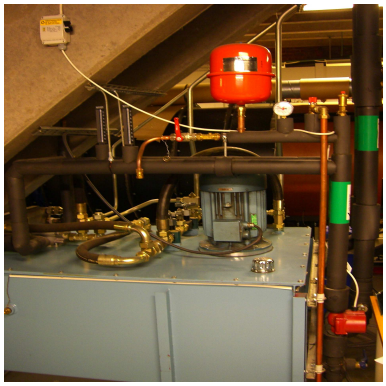

b)

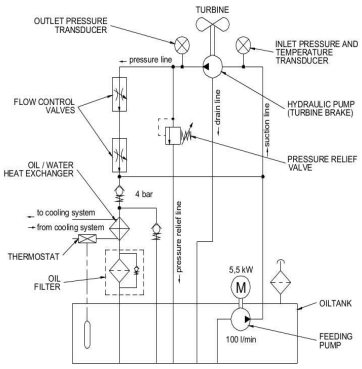

c)

d)

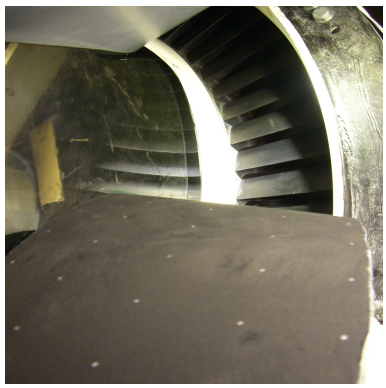

Figure 3.3: Hydraulic brake system. In figure a) can be seen the deposit of oil, the heat exchanger and the oil pump. In picture c) can be seen the controller of the fan that provides the flow into the HPT. Picture d) is taken from the vane surface that is used for the experiment. The blades of the HPT can be seen upstream of the vane.

3.3 Intermediate Turbine Duct

The other part which is very important inside the facility is the intermediate turbine duct (ITD). It was designed by Volvo Aero Corporation. It is specially designed to have a short length and at the same time minimize the pressure loss. The duct inlet has the same dimensions as the turbine outlet, because the match at that point. The area ratio (outlet/inlet) is 1.9, non-dimensional length (length/inlet height) of 7.27 and an aspect ratio (length/change in mid-radius) of 4. In Fig.3.4 can be seen a good scheme of the ITD. This duct is made of carbon fiber composite. The tolerances for the geometry are ±0.5 mm for diameter and length. Once everything was assembled the tolerance for the position of the struts is estimated to be ±1 mm in the axial and azimuthal directions and their angle accurate with ± 1°.

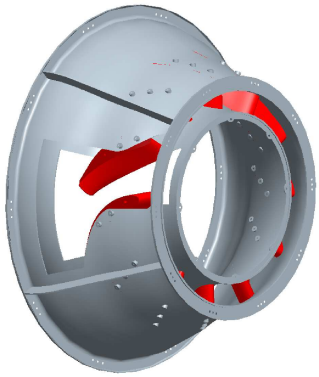

Figure 3.4: ITD with the hub and shroud window. These windows are very important for the optical access to obtain the images with IR-camera.

3.4 Traversing System

The traversing system is very important for creation the windows and for positioning the IR-camera. In both cases the 2 traversing systems were used. One of them is located external to the ITD. The configuration of this traversing system follows the shape of the shroud. The other traversing system is inside the duct (where there is no air flow). In Fig. 3.5 both traversing systems can be seen.

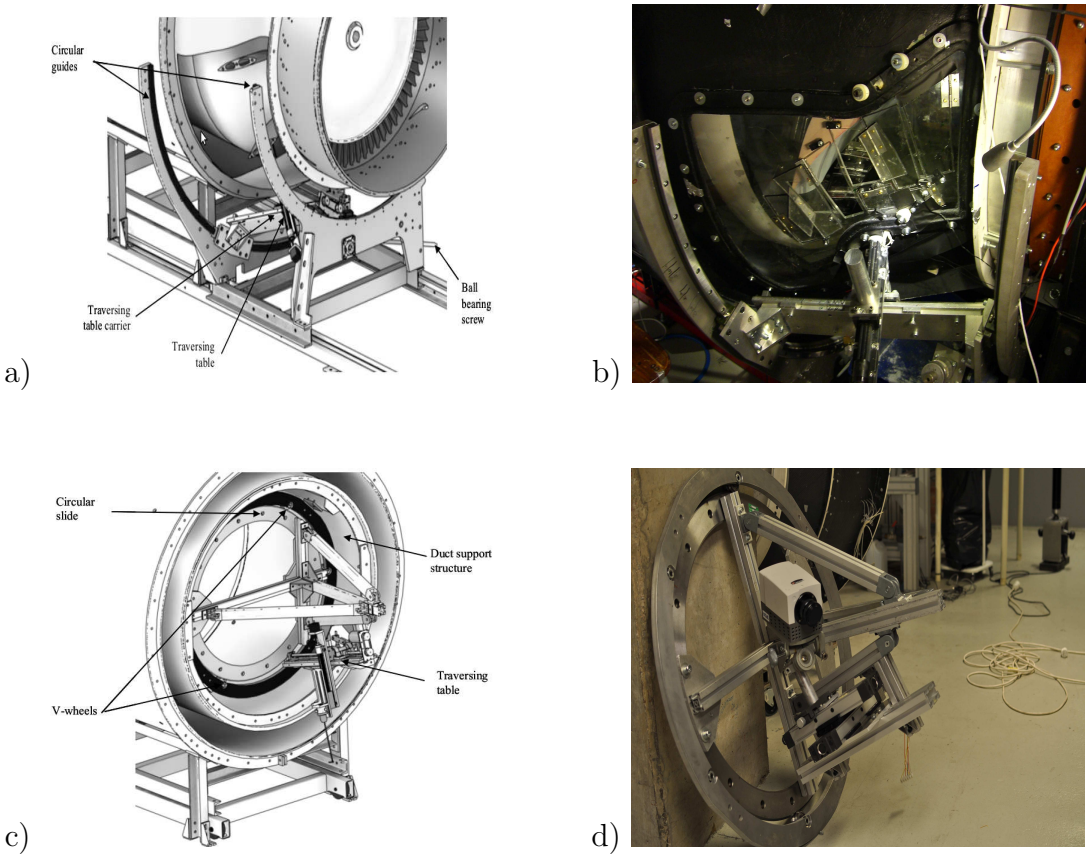

Figure 3.5: Picture a) and b) shows the "external" traversing system. Picture c) and d) shows the internal traversing system.

Both traversing systems perform movement in cylindrical coordinate system. The positioning is performed by a stepper motors and ball bearing screws and if it is necessary the camera position can be changed manually in order to have all the possible positions and view angles. The monitoring of these systems is done using by an inhouse software package written in LabView. All the motors are connected to a NI stepper motor controller, model MID-7604. This software uses cylindrical coordinates as can be seen in the Fig.3.6.

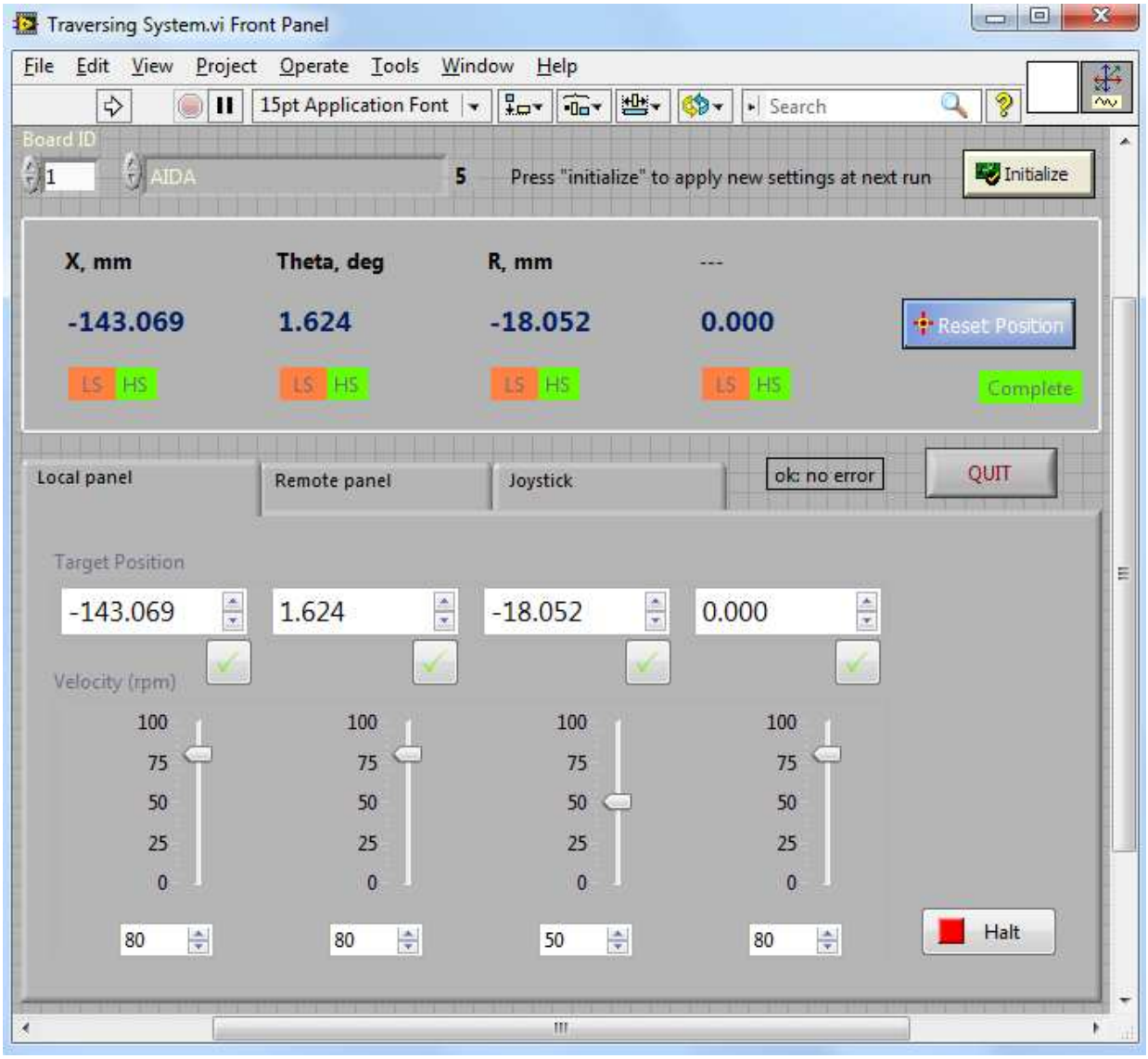

Figure 3.6: Monitorization of the traversing system.

Chapter 4

Setup for Measurements

In this chapter the procedures of experiment preparation and the assumptions which have been done for modeling the experiment are described. This chapter shows also the order of steps that have to be done in order to do the setup of the experiment.

4.1 Theoretical model

As it is described in chapter *Theoretical Backgrounds*, there are three heat transfer mechanisms involved. In this experiment the surface heat flux is measured, then it is not needed for the experiment setup to know the heat flux distribution inside the vane. The purpose for doing this experiment is to know the heat flux distribution along the surface.

The surface heat transfer mechanisms to the surroundings are convection and radiation. In order to explain the experiment and doing some calculation simplification Fig.4.1 represents a 1D case simplification of the actual experiment, which is a 3D case.

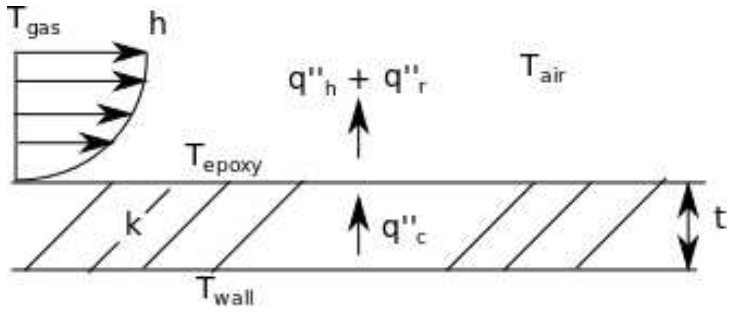

Figure 4.1: Simplification model for heat transfer measurement.[1]

As it can be seen in the figure above, there is conduction, convection and radiation heat transfer mechanism. The heat supplied to the epoxy surface by conduction is transferred to the surroundings via convection and radiation.

T_{wall} is the temperature of the aluminium core which is almost constant in the core due to the very high thermal conductivity (207 W/m·K). This can be seen in Fig. 1.4 and also in the validation path. The thermal conductivity k of silicone layer is approximately 0.22 W/m·K which is much smaller and creates big gradients of temperature.

T_{air} is the air far enough from the air boundary layer (T_{gas} is the boundary layer temperature distribution). It can be measured during the experiment. t is the wall thickness and it is theoretically 5 mm all around the vane, but due to the manufacturing process some "patches" can appear which change it. Anyway, it can be assumed that it is a constant value. T_{epoxy} is the temperature value that is measured with the IR-camera. Knowing this value the heat flux can be calculated in all the surface as it can be guessed looking at the next equations.

$$q''_c = -k\nabla T = \frac{k}{t}(T_{wall} - T_{epoxy}) \quad \text{Conduction heat flux} \tag{4.1}$$

$$q''_h = h\Delta T = h(T_{epoxy} - T_{air}) \quad \text{Convection heat flux} \tag{4.2}$$

$$q''_r \approx \sigma(\varepsilon_{epoxy}T^4_{epoxy} - \varepsilon_{air}T^4_{air}) \quad \text{Radiation heat flux} \tag{4.3}$$

Where ε_{epoxy} is dependent on the surface material (in this case, the black coating with ε_{epoxy} is equal to 1) and ε_{air} is the total emissivity of the surroundings which is very low. Applying energy conservation equation looking at the Fig. 4.1 the next equation is obtained.

$$q''_c = q''_h + q''_r \tag{4.4}$$

Assuming that the q''_r is neglectable due to the fact that it represents less than 10% of the second term in equation 4.4:

$$\frac{k}{t}(T_{wall} - T_{epoxy}) = h(T_{epoxy} - T_{air}) \Rightarrow h = \frac{\frac{k}{t}(T_{wall} - T_{epoxy})}{(T_{epoxy} - T_{air})} \tag{4.5}$$

This equation is very useful for validating that the 1D case and the 3D case calculations are more or less the same (In between 10% difference).

4.2 Black coating

It is very important for the experimental measurement to have a black body radiation surface in order to maximize the precision of the camera.

Unfortunately, the material of the vane is not a black body. Then it is necessary to apply a surface treatment which will provide the surface of the vane the properties of a blackbody. In order to achieve this surface properties Nextel Vetel-Coating 811-21 from Mankiewicz Gebr. & Co was used. The most important characteristics of this black coating are the very high emissivity (0.973) and the independence of the emissivity with the angle (almost diffuse radiation). The specifications of this coating can be seen in Table 4.1

Physical Property	Value	Comment
Total emissivity	973	Constant for our temperature range
Maximum angle for constant emissivity	30 deg	60º for 1% drop
Thermal conductivity	0.2 W/mK	Constant for our temperature range

Table 4.1: Nextel Vetel-Coating 811-21 specifications.[1]

It is important to point out that the thermal conductivity of the coating is almost the same as for the silicone and that the coating thickness was measured approximately 0.1mm.

4.3 Vane Surface Markers

After painting the vane with the special black coating it is possible to measure the temperature anywhere along the vane surface, but it is not possible to know just taking a picture which one is exactly the coordinate any point in a infrared image. In order to fix this problem, the vane was painted with marks that are visible with the IR-camera and they are not big enough to lose too much temperature information. Hence, the vane was painted with a silver marker which emisivity is different from the black coating emisivity and because of this, the marks can be seen in a IR image (see Fig. 4.2).

a) 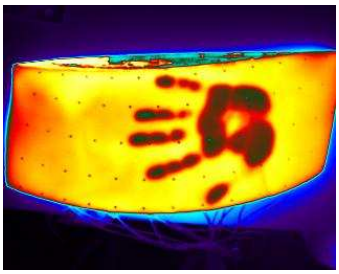 b) 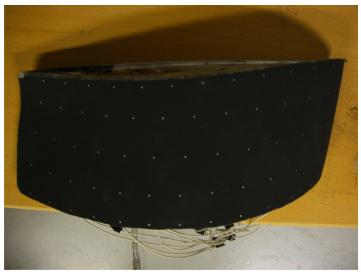

Figure 4.2: a) Picture with a standard camera. b) Picture with the IR-camera

The following paragraphs describe sequence that was done for making these dots.

First of all, a digital the vane model is needed. This model was done using CAD. There are several ways to extract point coordinates from a known geometry, but the one that was used is using ANSYS ICEM CFD software. This software is very useful to create the mesh of the vane and at the same time to extract points due to a user-friendly interface for this task.

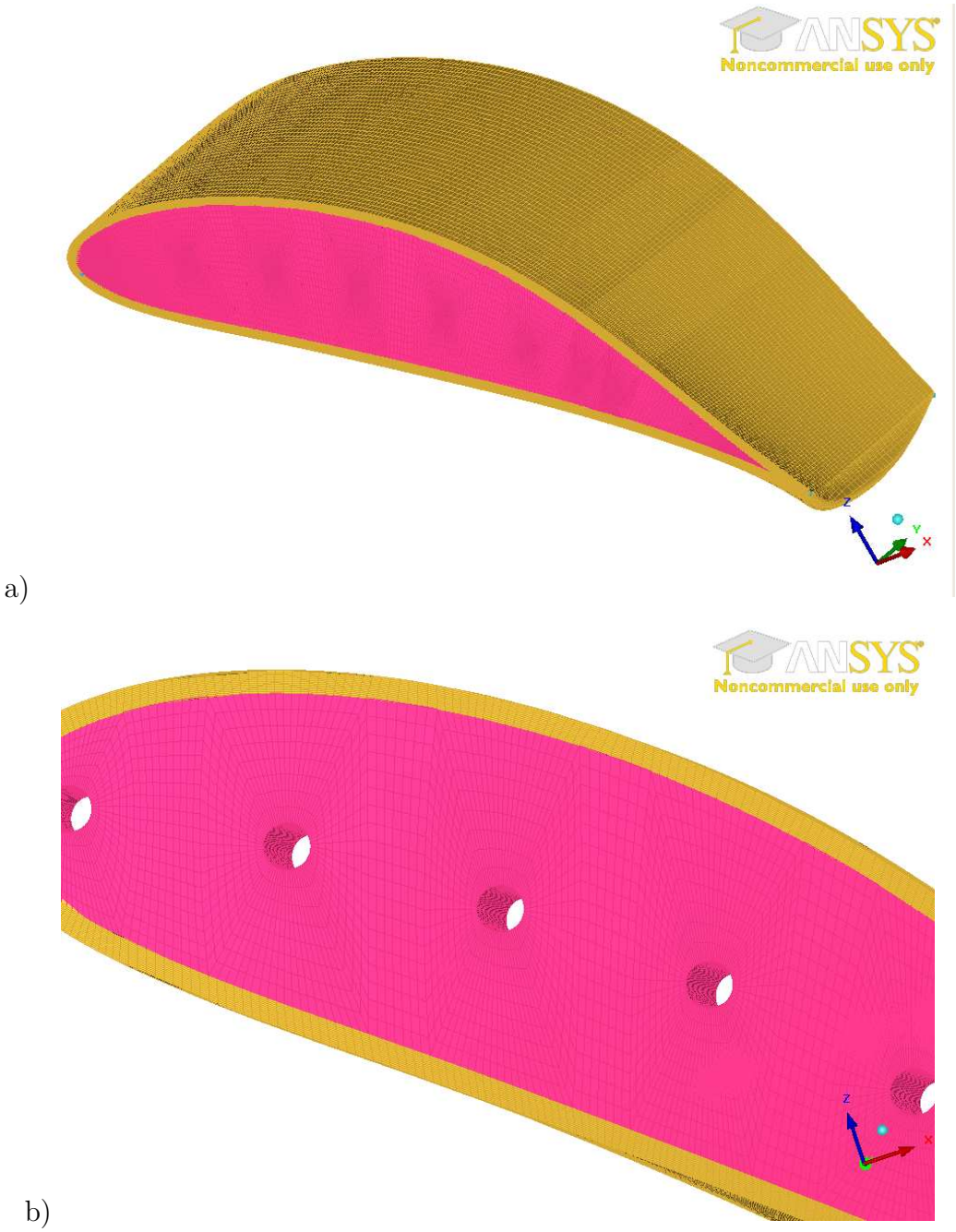

a)

b)

Figure 4.3: CAD design in ICEM. The mesh is included in the image.

First, it is needed to define over the shell 5 curves which are located at 5%, 25%, 50%, 75%, 95% between the side edges. Fig. 4.4 shows location of these curves.

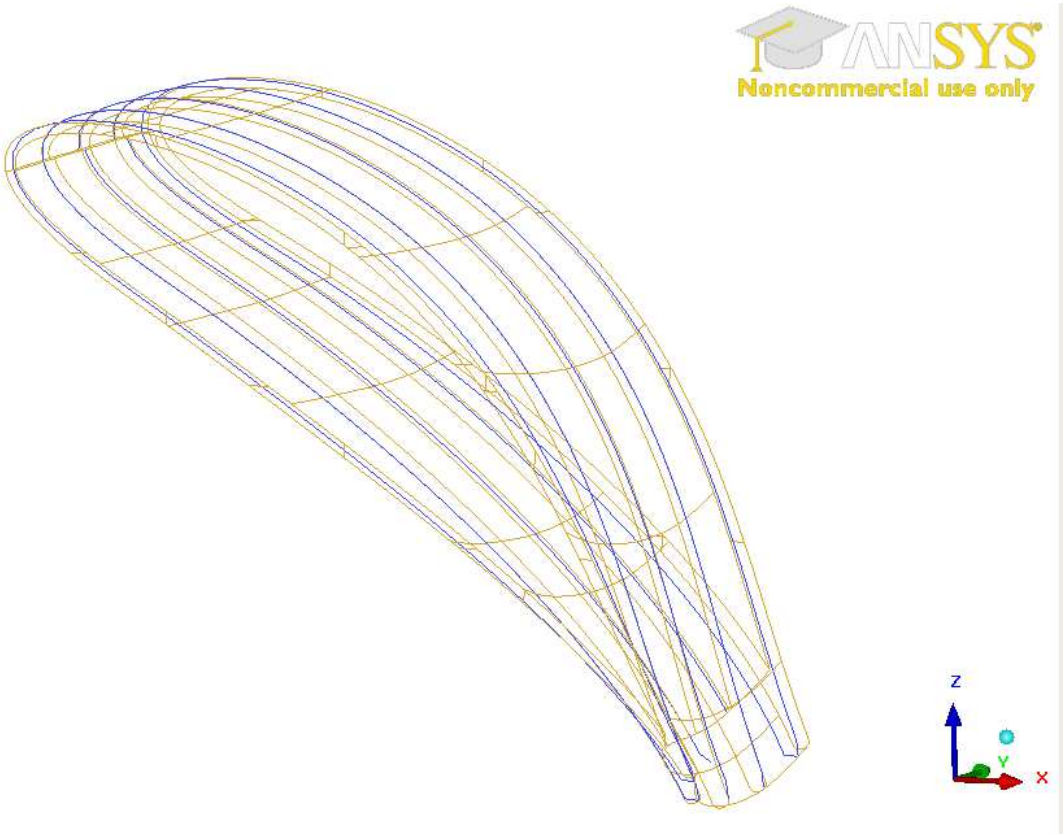

Figure 4.4: 5%, 25%, 50%, 75%, 95% curves.

The next step is to place on each curve 13 points equidistant. Then a total of 65 points can be seen in Fig 4.5.

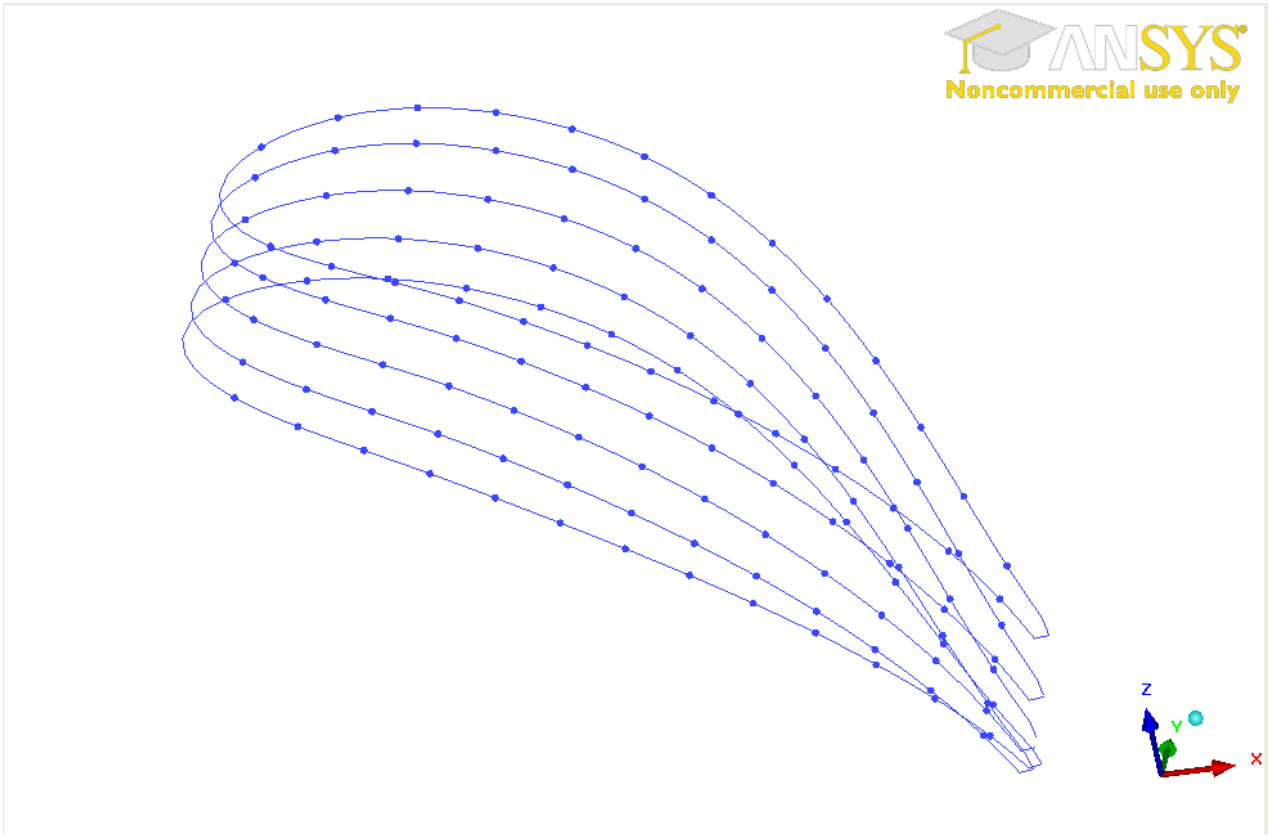

Figure 4.5: Marks over vane geometry and curves.

Now, importing this data into a *geometry* file with only a map of points can be done as it can be seen in Fig. 4.6.

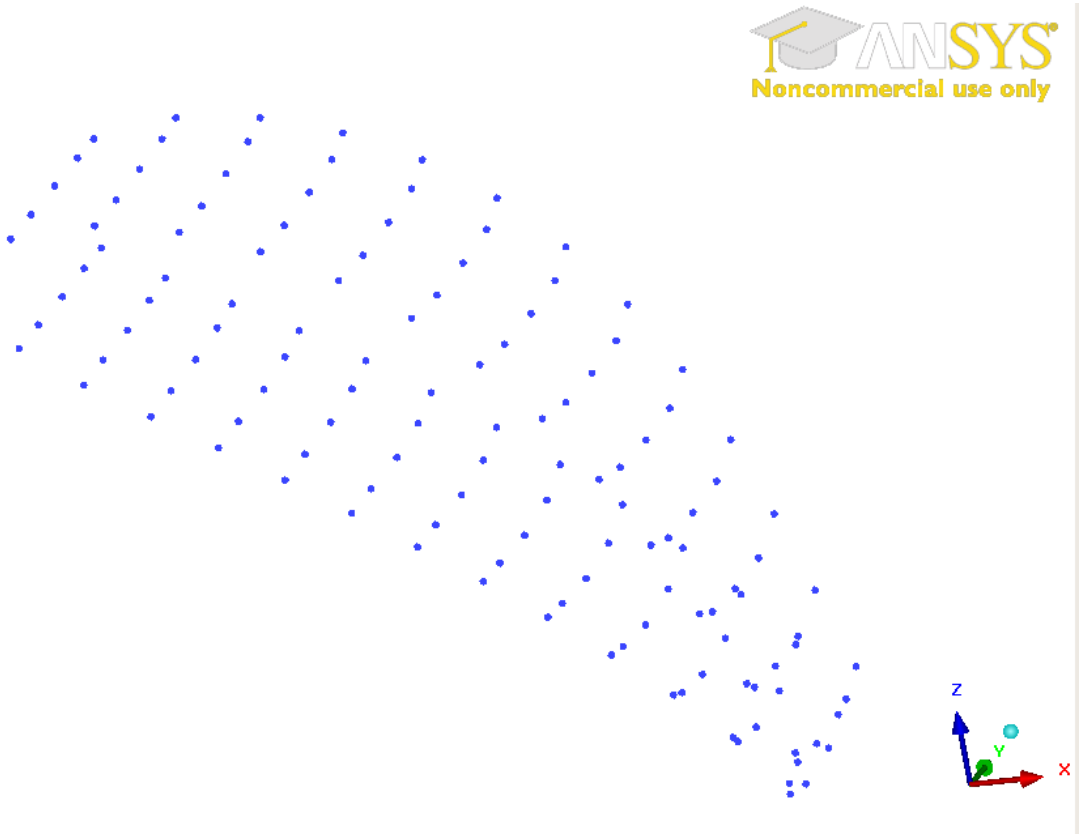

Figure 4.6: Markers over vane geometry.

Once this map of marks is done, it is possible to open the *geometry* file as an Excel file. Having all the physical coordinates of the points it is possible to create the marks. Although one question suddenly appears, which is the coordinate system that ICEM is using? How can I make the markers with a precision up to 0.01mm?

The answer to these questions is more difficult than they look like. First of all, in order to do the markers a traversing system was used having Cartesian coordinates as it can be seen in Fig. 4.7. This traversing system was assembled by us.

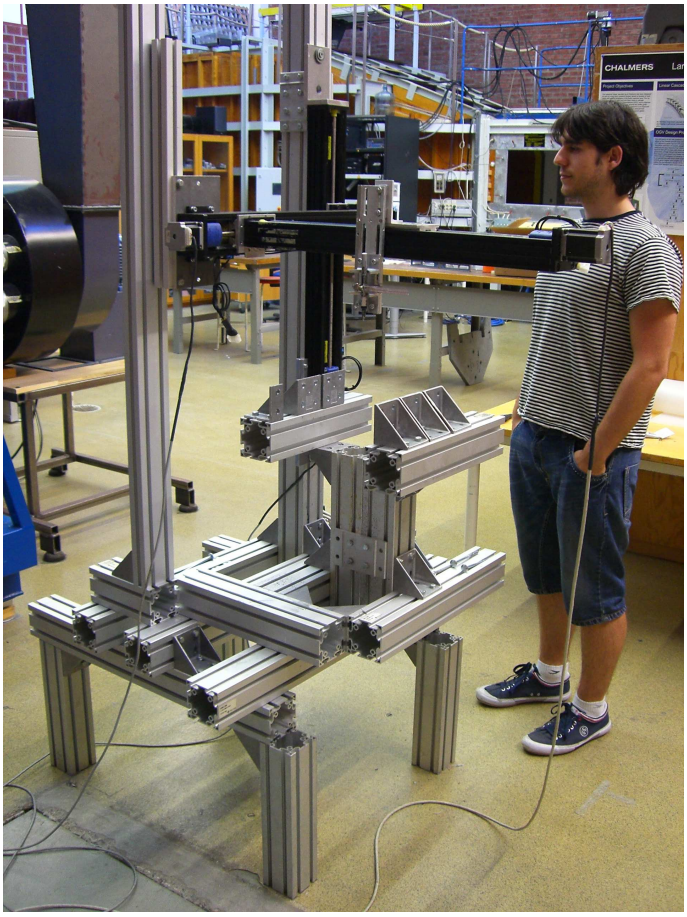

Figure 4.7: Traversing system for the markers.

Afterwards, the next problem that has to be solved is the unknown coordinate system. The way to fix this problem is plotting these points in Matlab and then rotates the vane markers in order to see in Matlab exactly the same vane position and orientation as in the traverse system (physical coordinates). Rotating the vane markers is done applying lineal transformation matrix for rotation. The comparison between the non rotated and the rotated markers can help to understand how the Matlab image fits with the reality (See Fig. 4.9)

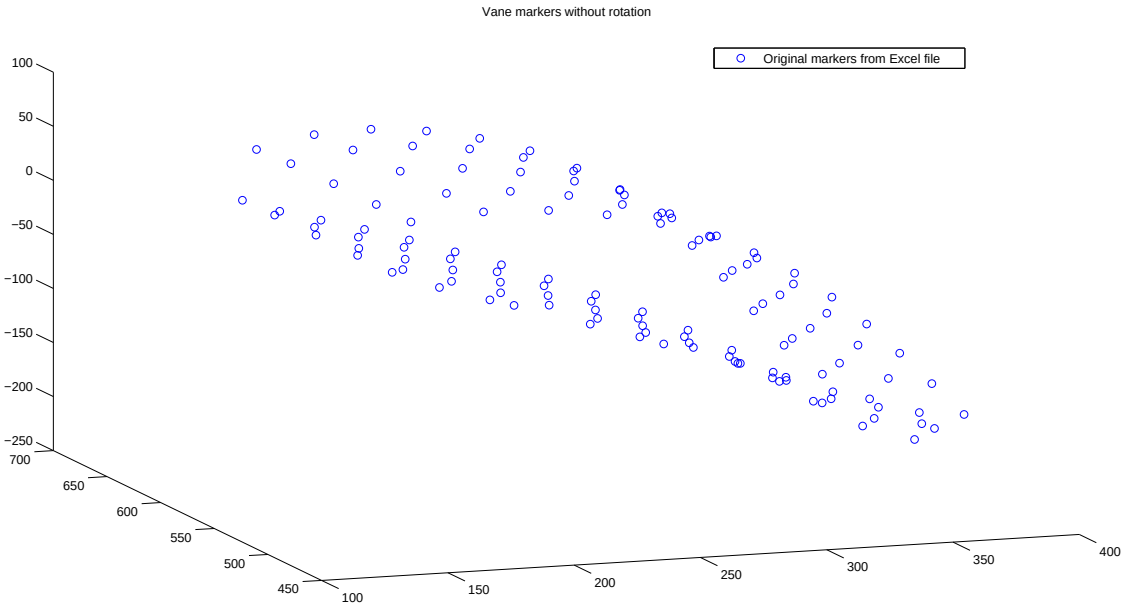

a)

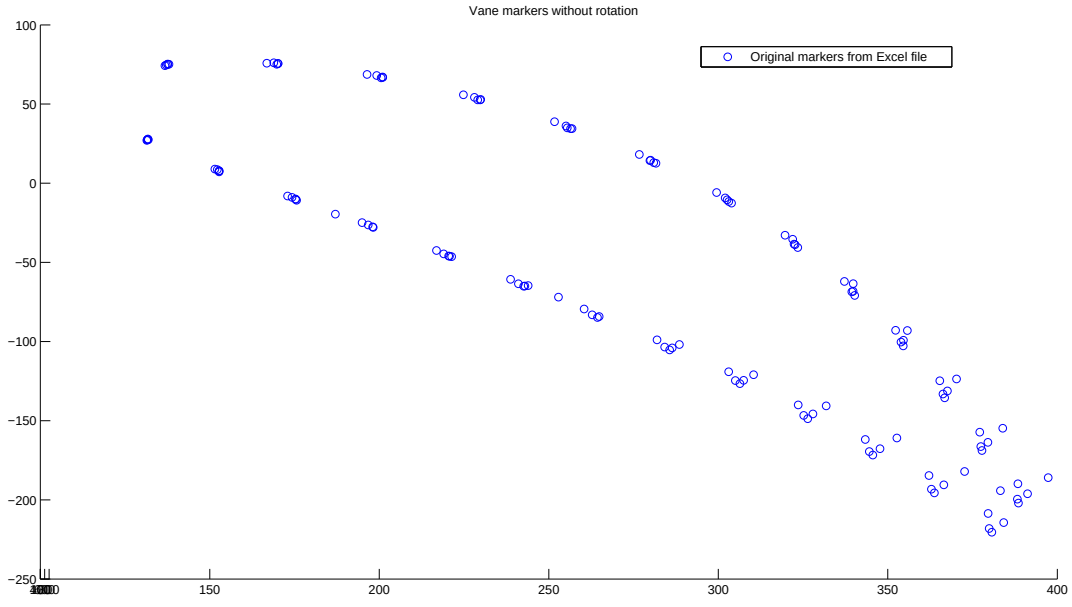

b)

Figure 4.8: Original markers visualized with Matlab. It is important to point out that the vane is not parallel with the XY plane.

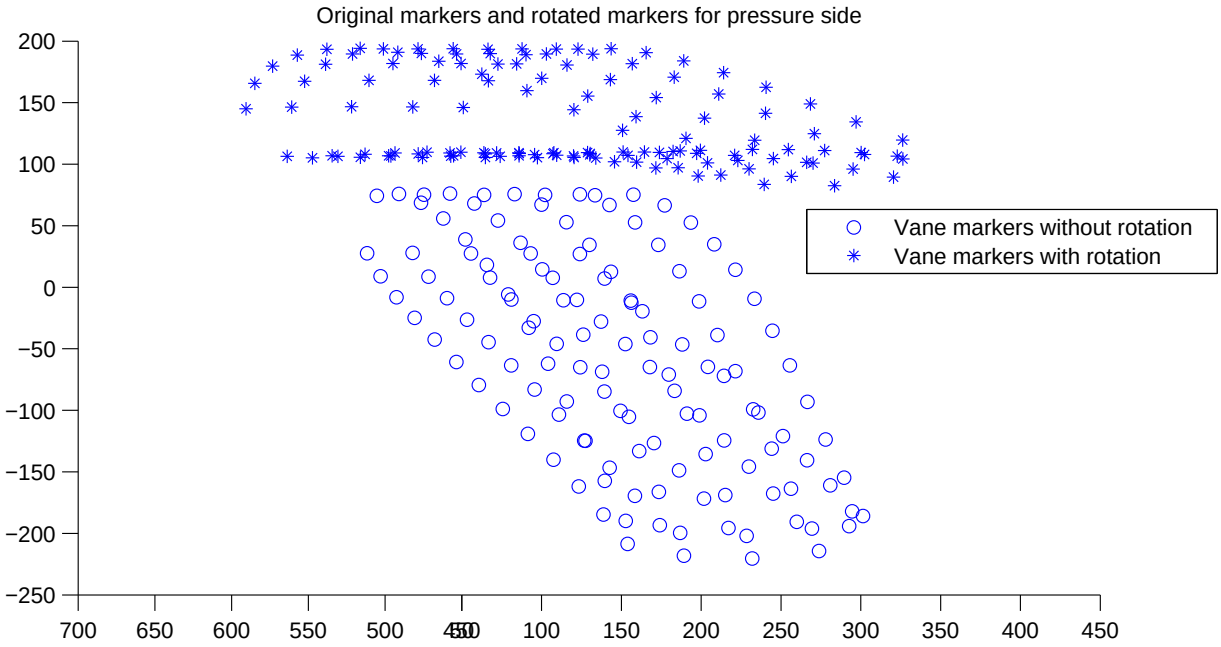

a)

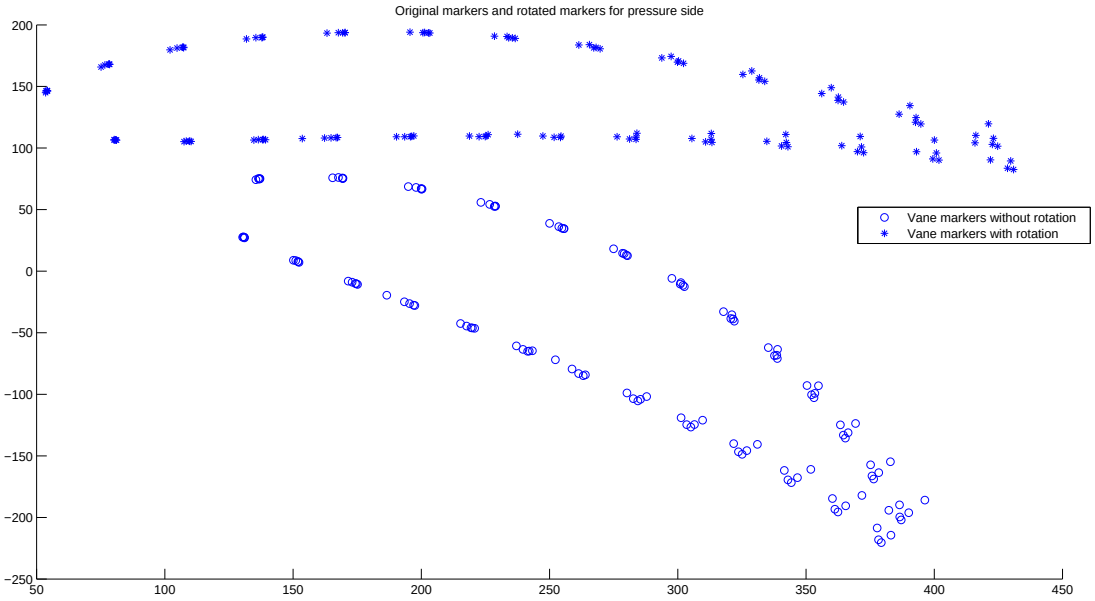

b)

Figure 4.9: Original and rotated markers visualized with Matlab. This was used to make the markers of the suction side.

Looking at Fig. 4.9 it is possible to see that the rotation made the vane parallel to the XY plane. It can be guessed that the XY plane in Matlab is the same as the one in our traverse system, then it is known that this is close to be in the right position. The last step is to check if the traverse coordinate system is perfectly matching with the Matlab coordinate system. This process has to be done manually using some physical reference points of the vane. In this case, it was used the corner points of the aluminium core trailing edge and the corner points of the silicone shell leading edge. Knowing the coordinates of these points, if the coordinate systems are right it is supposed to be possible to go from one reference point to the other just using the traverse system coordinates. If the marker is over all the reference points without changing the coordinate system, it means that Matlab and physical traverse system are same. Then, it is possible to put the markers and the vane will be prepared for the experiment.

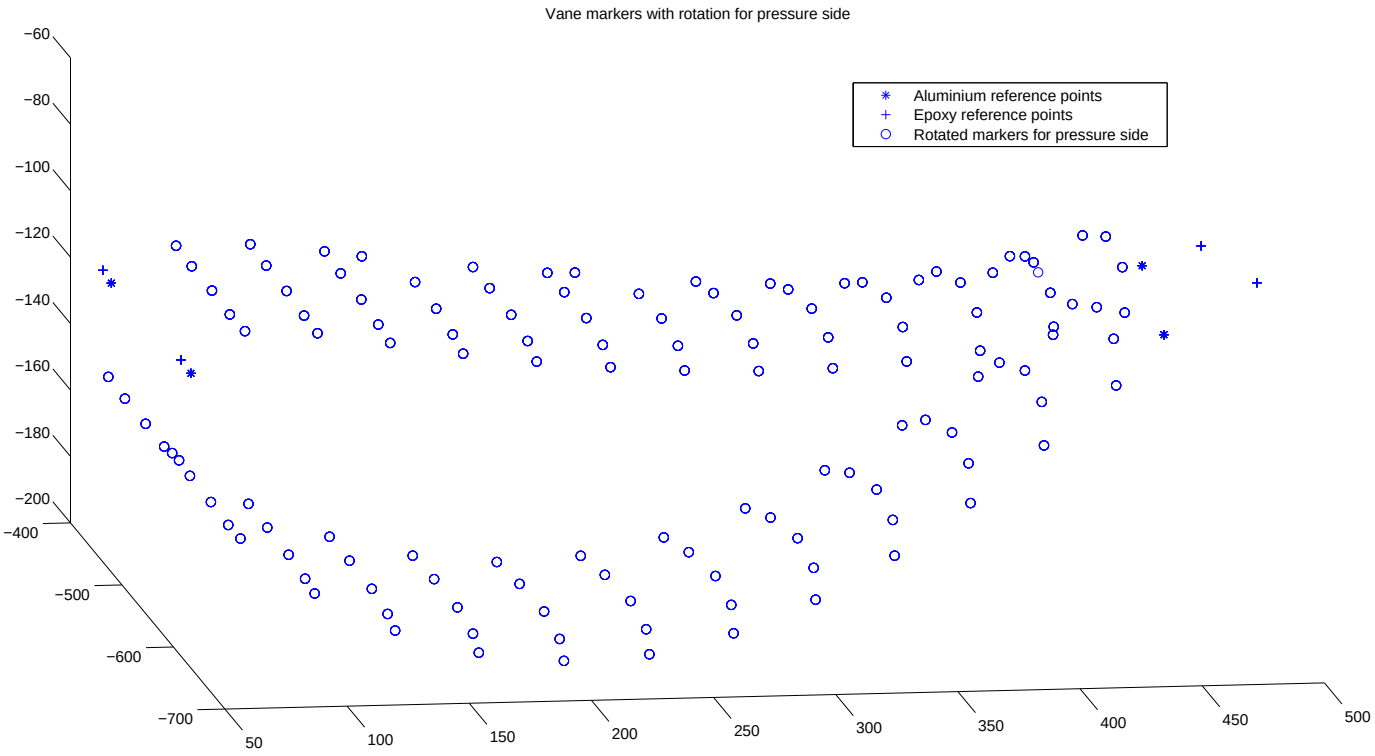

Figure 4.10: Markers with reference points.

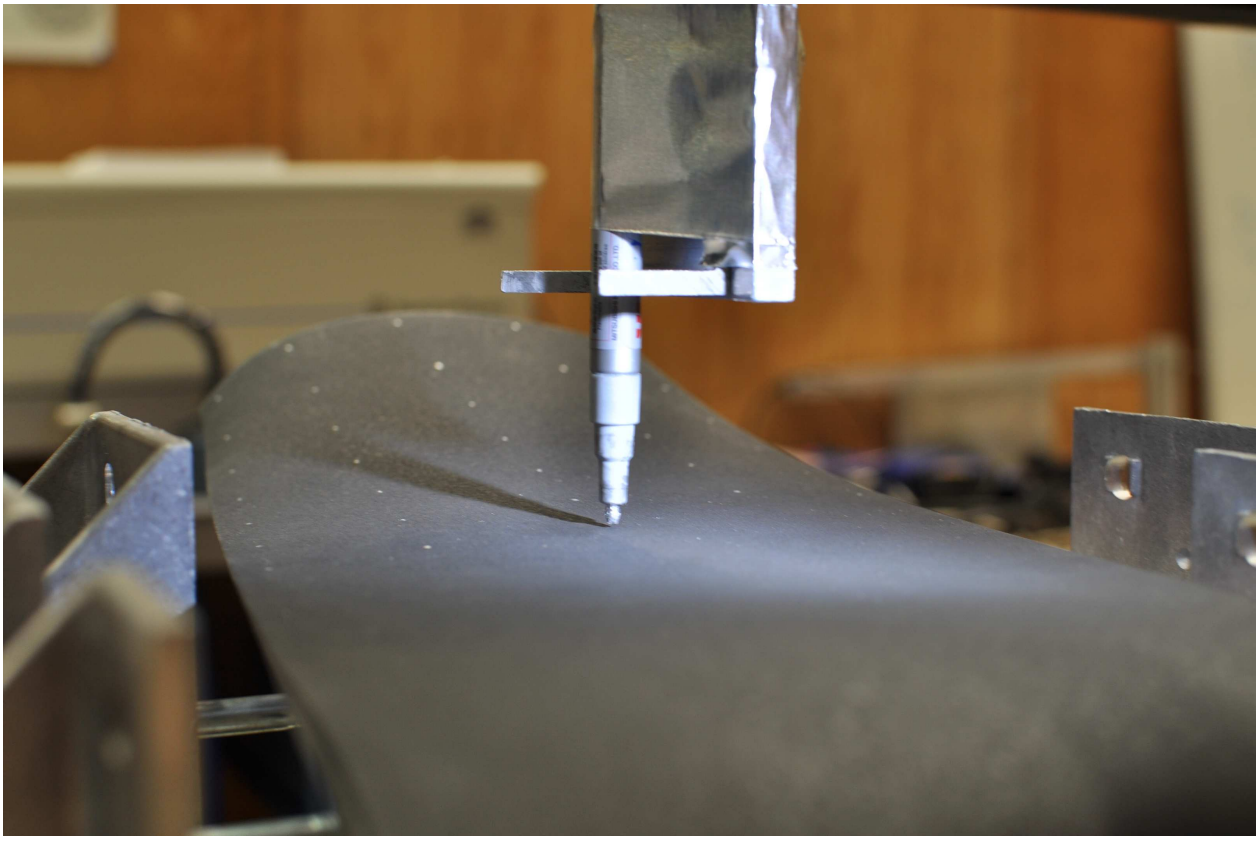

Figure 4.11: Picture taken while doing markerss.

4.4 Camera Setup

The IR-camera is a MWIR Phoenix Camera System. The resolution of this camera is 320x256 and the specifications can be seen in Table 4.2.

Manufacturer	Flir Systems Inc.
Model	Phoenix MWIR Camera System
Detector type	Indium Antimonide
Detector spectral response	1 µm - 5.4 µm
Filtered spectral response	3 µm - 5 µm
Format (pixel number, HxV)	320 x 256
Detector pitch	30 µm
Detector cooling	Stirling cycle
Detector temperature	77 K
Dynamic range	14 bit
Noise equivalent temperature difference (sensitivity)	25 mK
Minimum window	2 rows x 4 columns
Integration mode	Snapshot
Max frame rate full window	122 Hz.
Max frame rate minimum window	13.6 kHz
Integration time	9 µs - 16.6 ms
Output	Composite video / digital image / RS.232 camera control
Input	Sync (arm/trigger) / RS 232 camera control
Optics	25 mm f/2.3 MWIR / Janos Technology

Table 4.2: Camera Specifications.[9]

Then, it is very important to be careful with the camera configuration because the precision of the experimental results will be dependent on this.

First of all it is necessary to optimize the integration time and gain levels in order to maximize the resolution of the camera. Due to the maximum level of counts is approximately 16000 counts, the hot source (maximum temperature that is going to be achieved during the experiment) should be measured 5°Chigher than the maximum temperature. Afterwards, the integration time is set looking at the number of counts when the camera is imaging at hot source. The device used for camera calibration can be seen in Fig. 4.16.

Afterwards, the two-point non-uniformity correction (NUC) is done. The main reason to do this is to obtain the same temperature in all the pixels when the camera is pointing at a uniform temperature source, then it will be possible to equalize all the pixels when it is pointing at a non-uniform temperature source. Then, it will be necessary to use 2 uniform temperature sources, one at approximately 12000 counts (75% of the maximum counts) and the cold source will be an aluminium plate at room temperature painted with the black coating (See Fig. 4.17). For the hot source will be used the tool that can be seen in Fig. 4.16. In order to perform the non-uniformity

correction (NUC) RDac was used for controlling the camera. Looking at the Fig. 4.12 it can be seen how it is possible to do the NUC.

a) 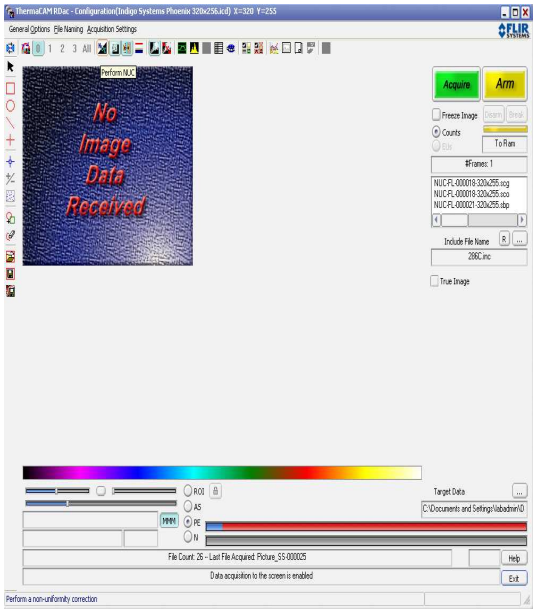

b) 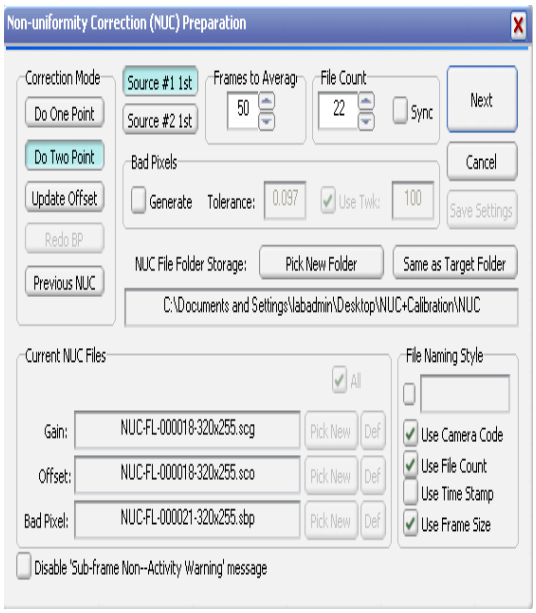

Figure 4.12: NUC with RDac.

The result of NUC can be seen in Fig. 4.13

a) 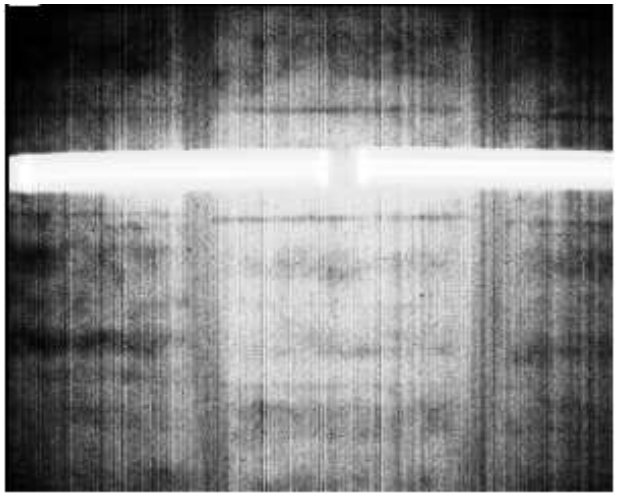

b) 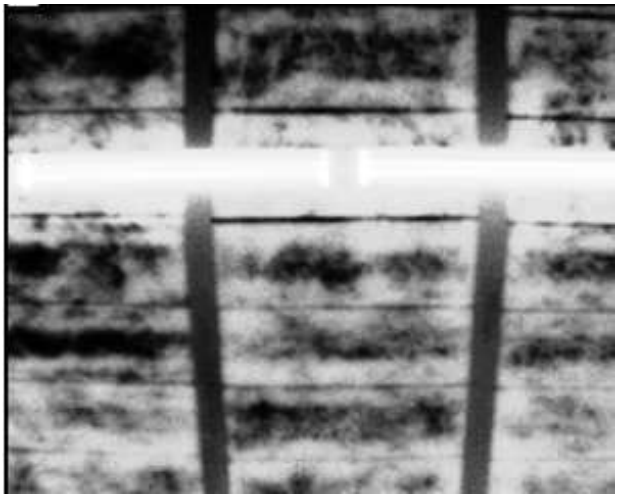

Figure 4.13: a) Picture taken without NUC. b) Picture taken with NUC.

After the NUC correction, it is convenient to correct the bad pixels that can appear in the image. This bad pixels can be seen that are totally out

of range. For example, the maximum temperature in a picture is 30℃ and these bad pixels measure 70℃. Then, in order to eliminate these bad pixels that are always in the same position the RDac bad pixel detector is used. Introducing some conditions for detecting bad pixel and separate them from errors producing by internal camera noise the map of bad pixels will be generated.

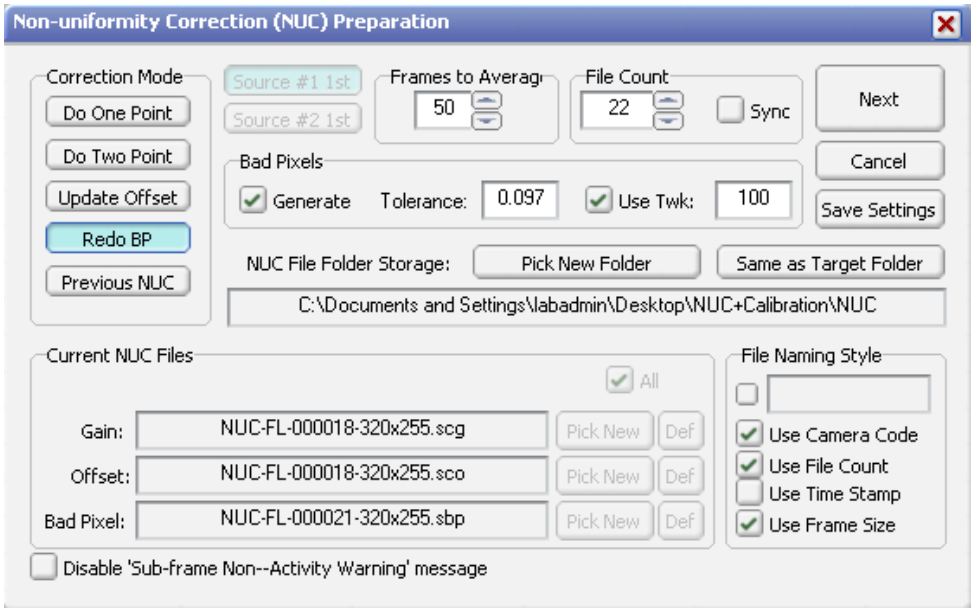

Figure 4.14: Cold source.

Therefore, it is necessary to transform the information given by the camera in counts to temperature. For this reason, it necessary to calibrate the camera with 5 uniform temperature sources in order to generate a 4^{th} grade polynomial of interpolation which will be used to calculate the temperature knowing the counts of each pixel. Then using the cold source again and the black box (Fig. 4.16) it is possible to perform the temperature calibration and to obtain the polynomial. To do this the software RCal is used.

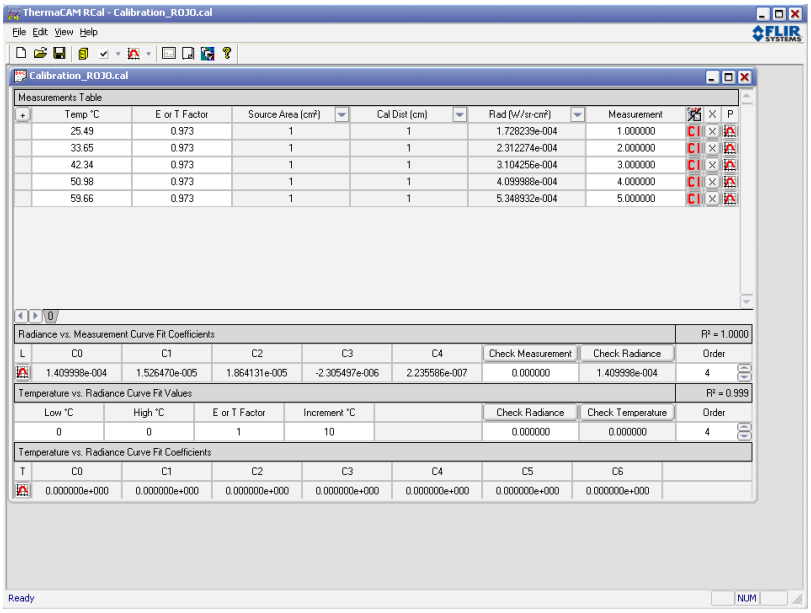

Figure 4.15: Calibration.

a)

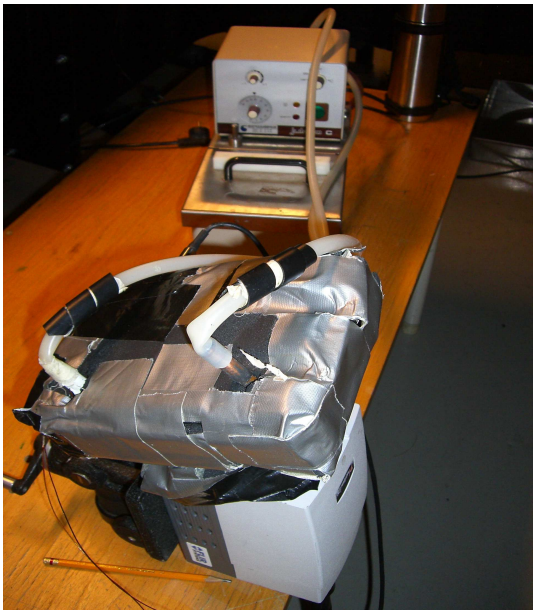

b)

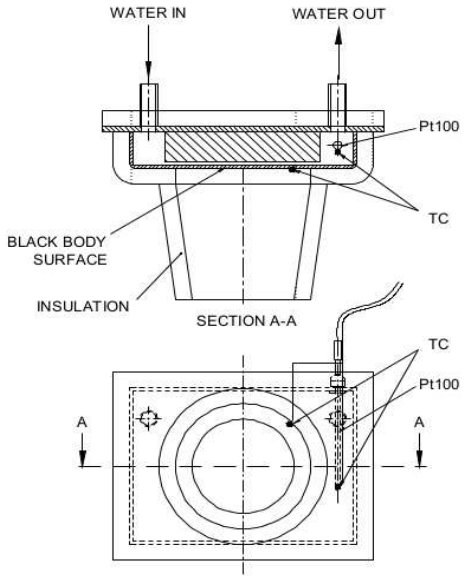

Figure 4.16: Black body used for camera configuration. It uses heated water circulation for temperature control and is painted with Nextel Velvet Coating. The water temperature is controlled with a PI temperature control. The precision of this device that uses Pt100 and thermocouples to control the temperature is approximately 0.1℃.[1]

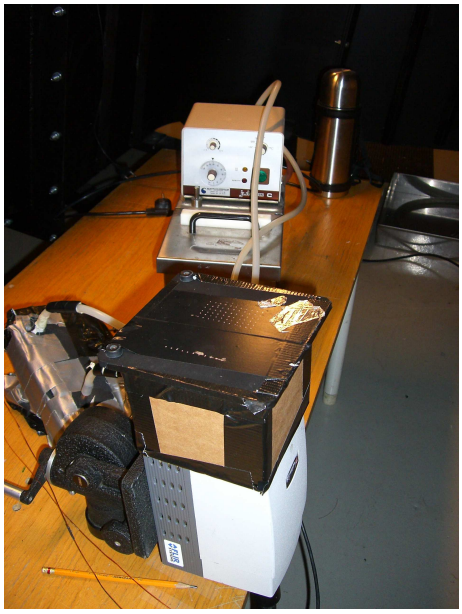

Figure 4.17: Cold source.

4.5 Window Design

One of the most important part of the experiment setup is the optical access to the vane. IR-Camera imaging cannot be performed through the plexiglas the window due to this window has a very low transmissivity (in fact, the reflectivity is very high) at infrared spectrum. Then, it is needed to make some windows that are able during the experiment to be closed and just when it is needed, to be opened almost instantaneously in order to avoid temperature change in the vane.

First of all, it is necessary to fix the camera in all the positions and angles that are needed to take the pictures. During this procedure, some tape is used in order to mark all the frames of the pictures that had been taken. Fig. 4.18 is the result of this procedure in the outer window.

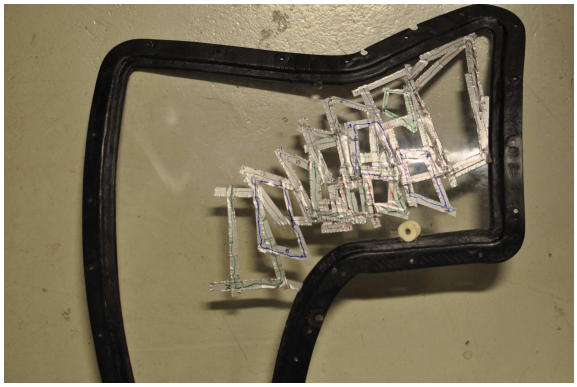

Figure 4.18: Frame of the windows.

Then, looking at all the frames, the design of the windows starts. It is very important to check that all the pictures can overlap and that it is possible to measure close to the edges. Afterwards, once it is decided on the shape and the size of the windows, using a driller with a 3mm diameter mill the window's holes will be made.

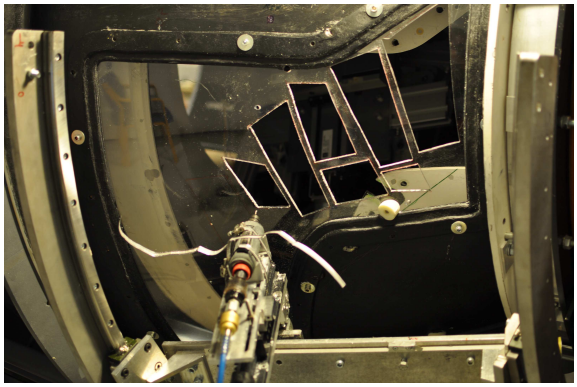

Figure 4.19: Window's holes.

It is also very important to make a rubber seals on the frames of the plastic windows as it can be seen in Fig. 4.20. This rubber will prevent flow leakage from the ITD to the room.

Figure 4.20: Window's holes.

Then, in order to open and close very fast these windows, a hinge is used with a spring. This spring is working while the window is closed due to a small lock avoids that the window will be open. Once this locker is turned, the window will be opened in short time.

Finally, all the attaching nuts are glued in order to avoid that any lock or hinge can be removed by the forces that can be applied. Fig.4.21 shows the final result of the outer window.

a) 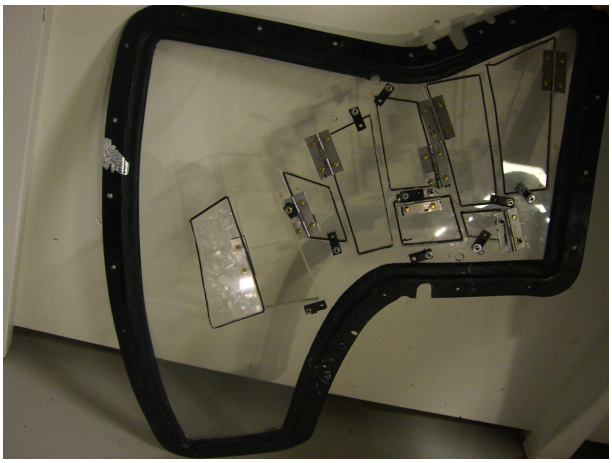 b) 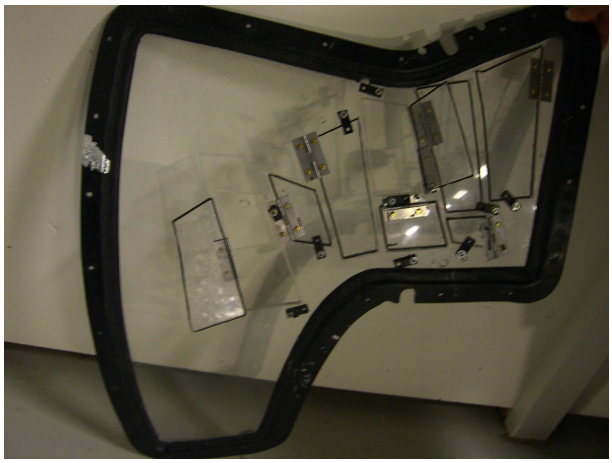

Figure 4.21: Window finished. It can be seen the window in the mdidle of the picture opened and closed.

Chapter 5

Results

5.1 Validation

First of all, it is important to check if the assumptions mentioned in section *Theoretical Model* are right in the simulations and during the experiment.

First of all, these were checked simulating the conditions that are predicted for the experiment. In order to know the boundary conditions, the power input that will be used for the experiment was measured. Then, the heat flux is calculated for the heater's boundary conditions. It is assumed that the convection heat transfer coefficient is 100 W/m^2K. Then, the result of this simulation can be seen in Fig. 5.1

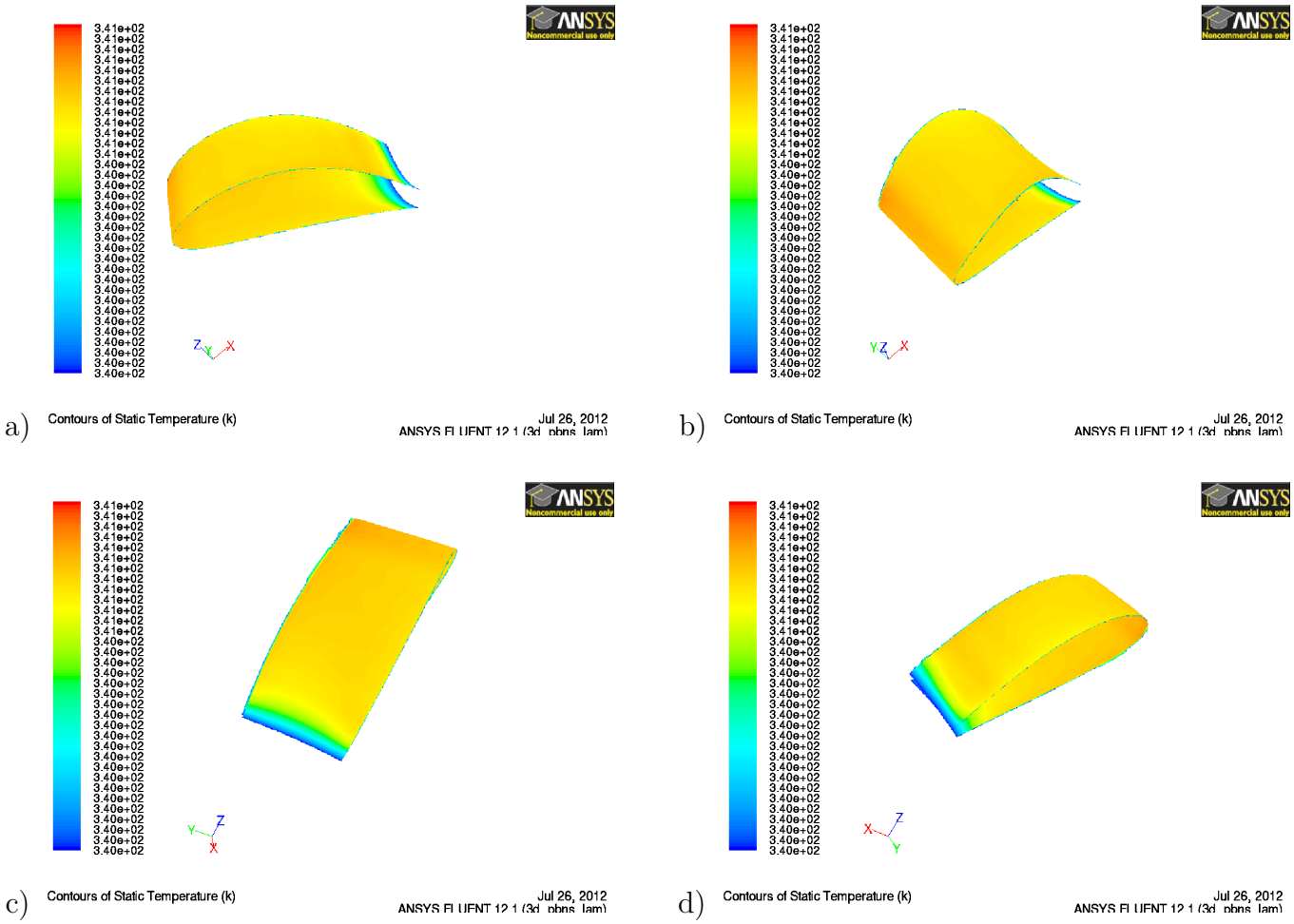

Figure 5.1: Results of numerical simulation using FLUENT for validation.

As it can be seen in Fig. 5.1 the maximum temperature difference along the aluminium surface is 1°C. Taken into account that this only happens in a very small area, it can be assumed that the aluminium core temperature is constant along the surface.

5.2 Post procesing

Once the infrared pictures are taken with the IR-camera it is needed to assembly them in order to have a complete and continuous map of temperature for pressure side and suction side. Matlab was used for the post proccesing. In order to explain all the steps, a picture from the pressure side will be used as example.

First of all, it is needed to know if the picture belongs to the pressure side or to the suction side in order to load the vane point coordinates from marker file. This fact will be explained deeper later. Then, the picture is a bidimensional temperature map where there is no information about the geometry that represents implicitly.

Furthermore, it is needed to filter the image in order to remove temperature data outliers. Basically, this filter is searching for peaks that have totally different temperature than the surrounding pixels. Afterwards, the result of these procedures can be seen in Fig. 5.2

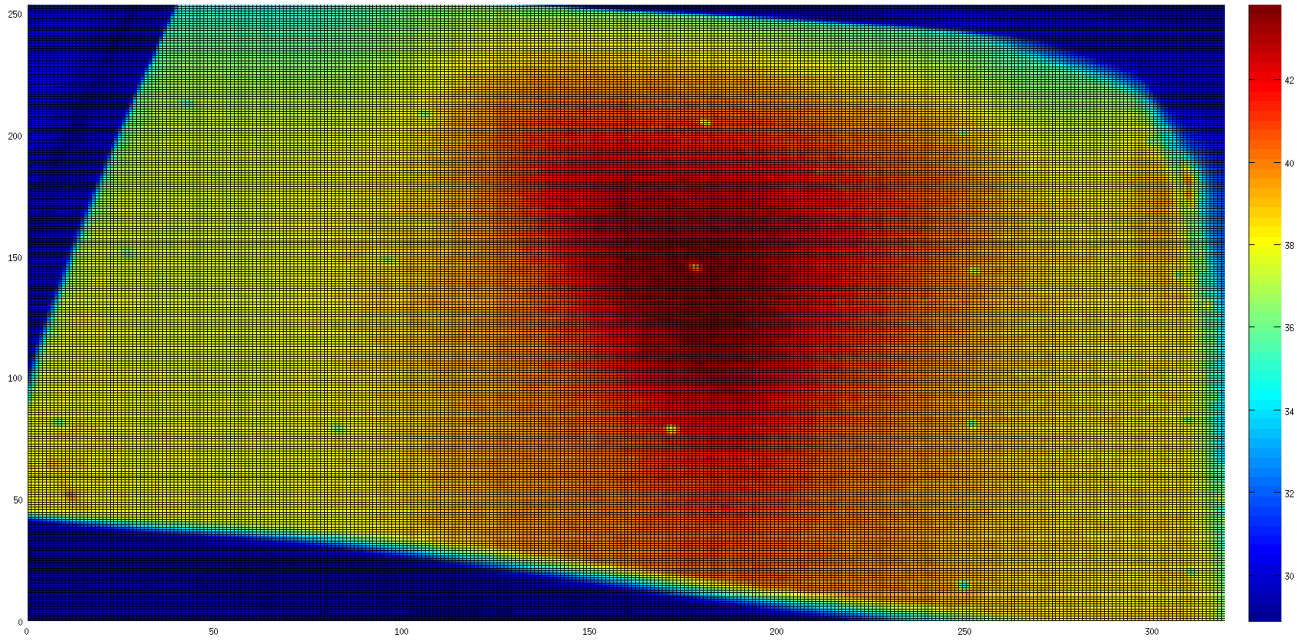

Figure 5.2: Temperature map after filtering.

Then, it is necessary to select the zone squares that will be extracted from the picture. This step is manual due to some of the images overlap. Afterwards, the silver markers that appear in the thermography as small points are removed using an interpolation method. This interpolation removes the points selecting the area manually and it uses as valid data the pixels surrounding this area. This method uses a 2D cubic interpolation. The result of this procedure can be seen in Fig. 5.3

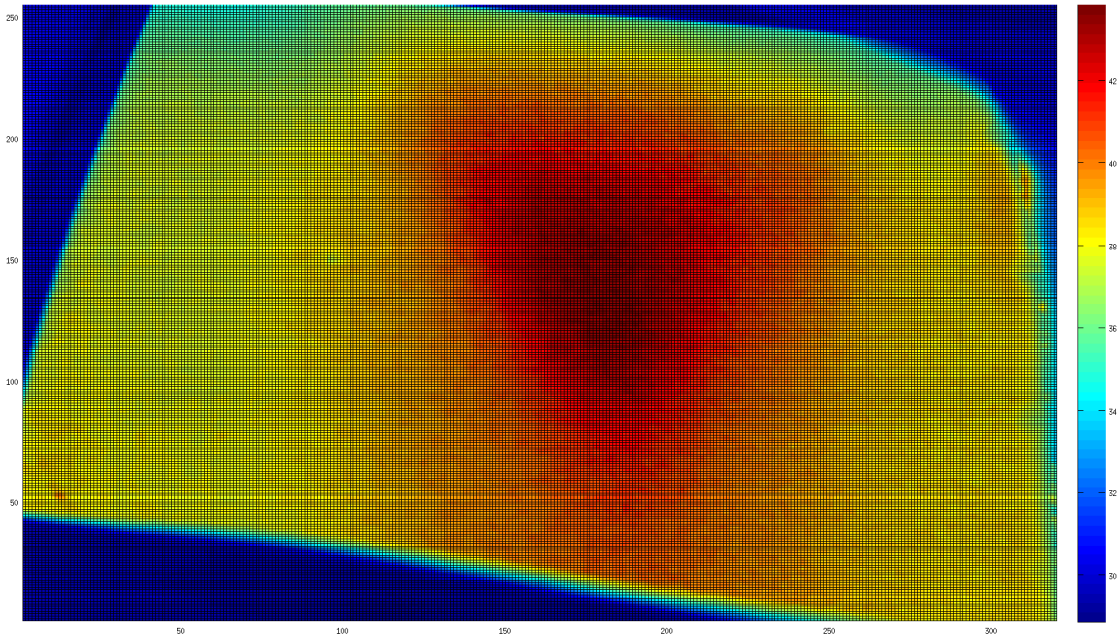

Figure 5.3: Temperature map after removing markers.

Afterwards, it is needed to transform this map of temperature into a 3D map of temperature which includes the real geometry. Then, the picture will be divided into the number of squares that are needed and each one will be analyzed individually.

First of all, a square is selected as can be seen in Fig. 5.4 using the markers as reference for the corners of the picture.

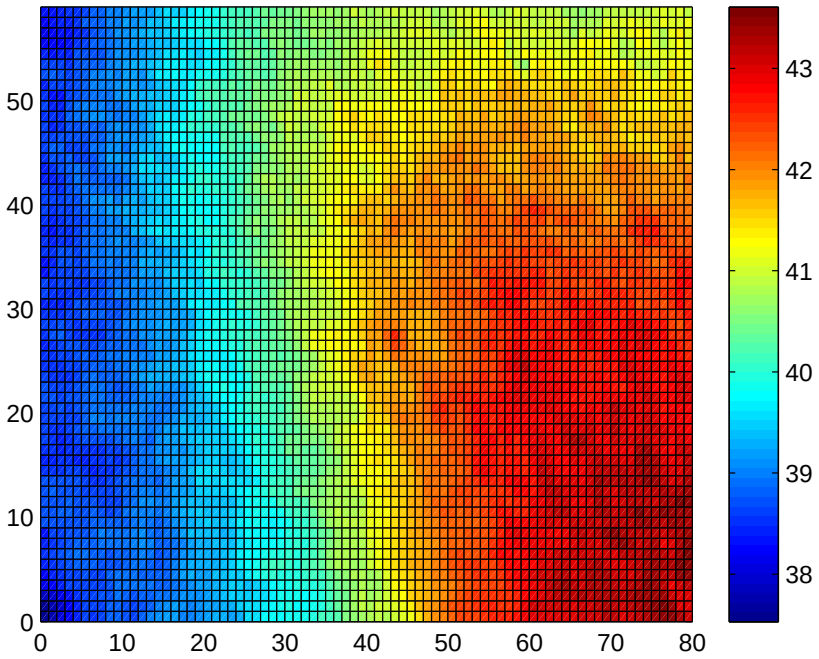

Figure 5.4: Temperature map of one square.

It is important to point out that even if the square in the original picture is not rectangular, it is rectangular after a transformation where the pixels change position and some of them are duplicate in order to not to lose information. If the removal of duplicate pixels is done, then it is possible to lose some pixels in this transformation.

Once this transformation is done, it is needed to set the coordinates of the corners of the Fig. 5.4. In order to do it, using the excel file where the coordinates of the markers are saved it is possible to obtain the geometry of this square using lineal interpolation in the sides of Fig. 5.4. The result of this procedure can be seen in the Fig. 5.6 and 5.5

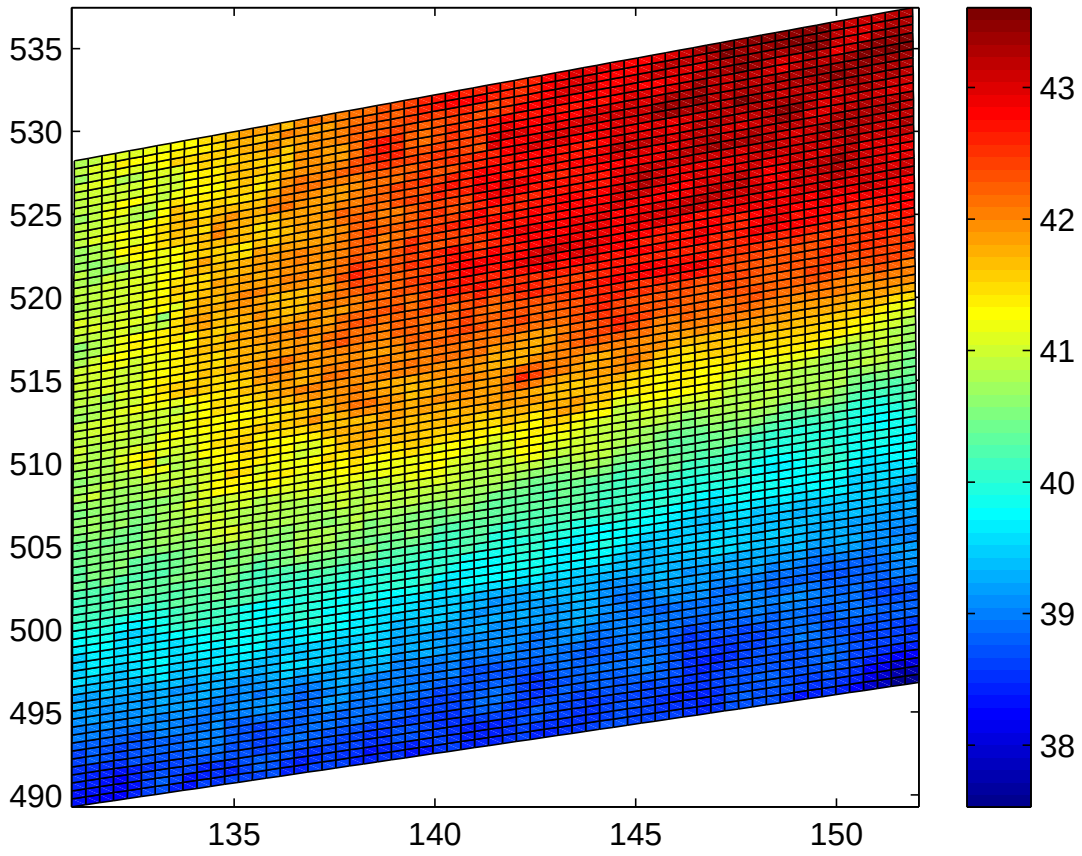

Figure 5.5: Temperature map of one square in xy real coordinates.

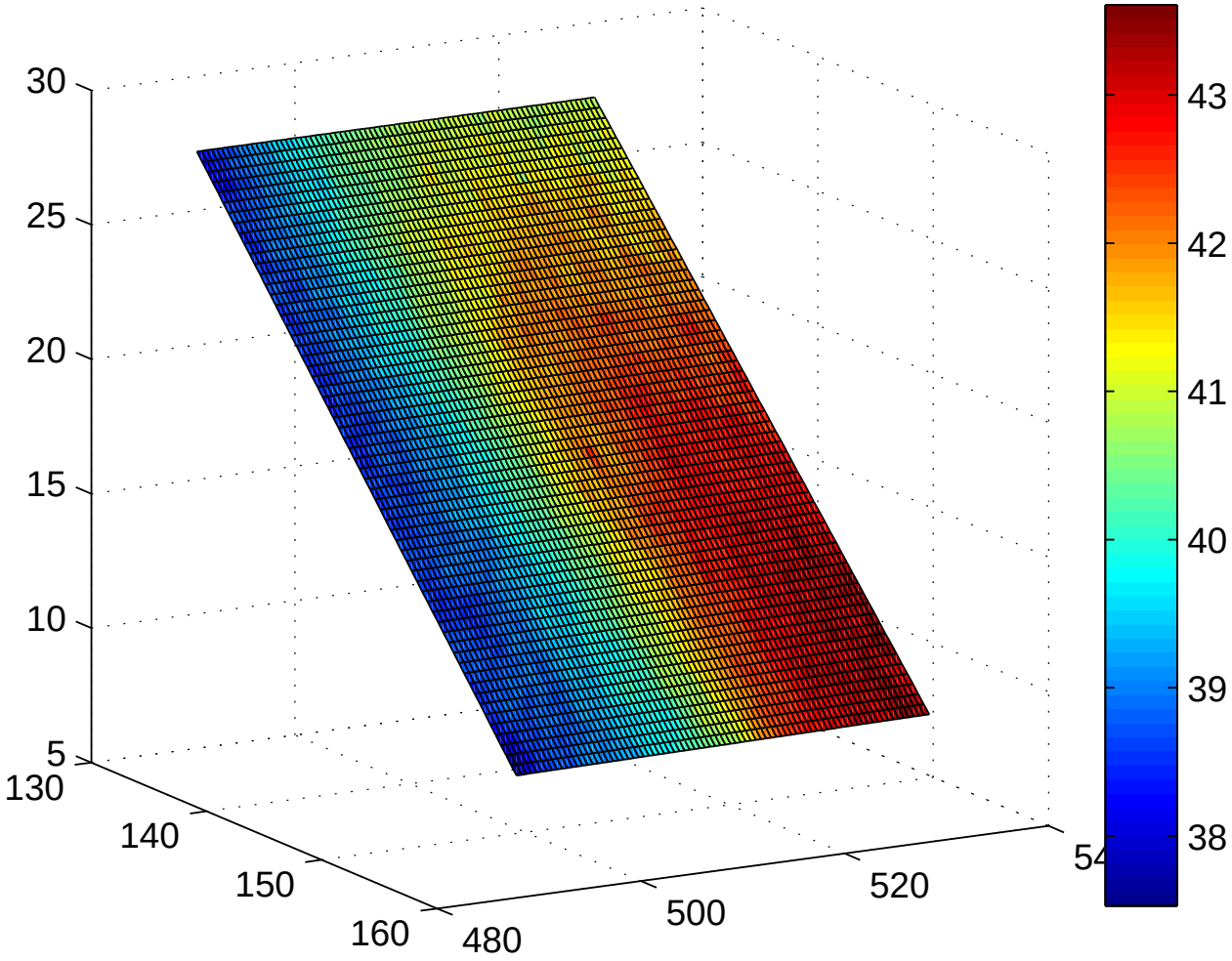

Figure 5.6: Temperature map of one square in xyz real coordinates.

Doing this procedure with all the squares that can be seen in Fig. 5.2 the next processing step is obtained in which one it is possible to see the last result of this procedure.

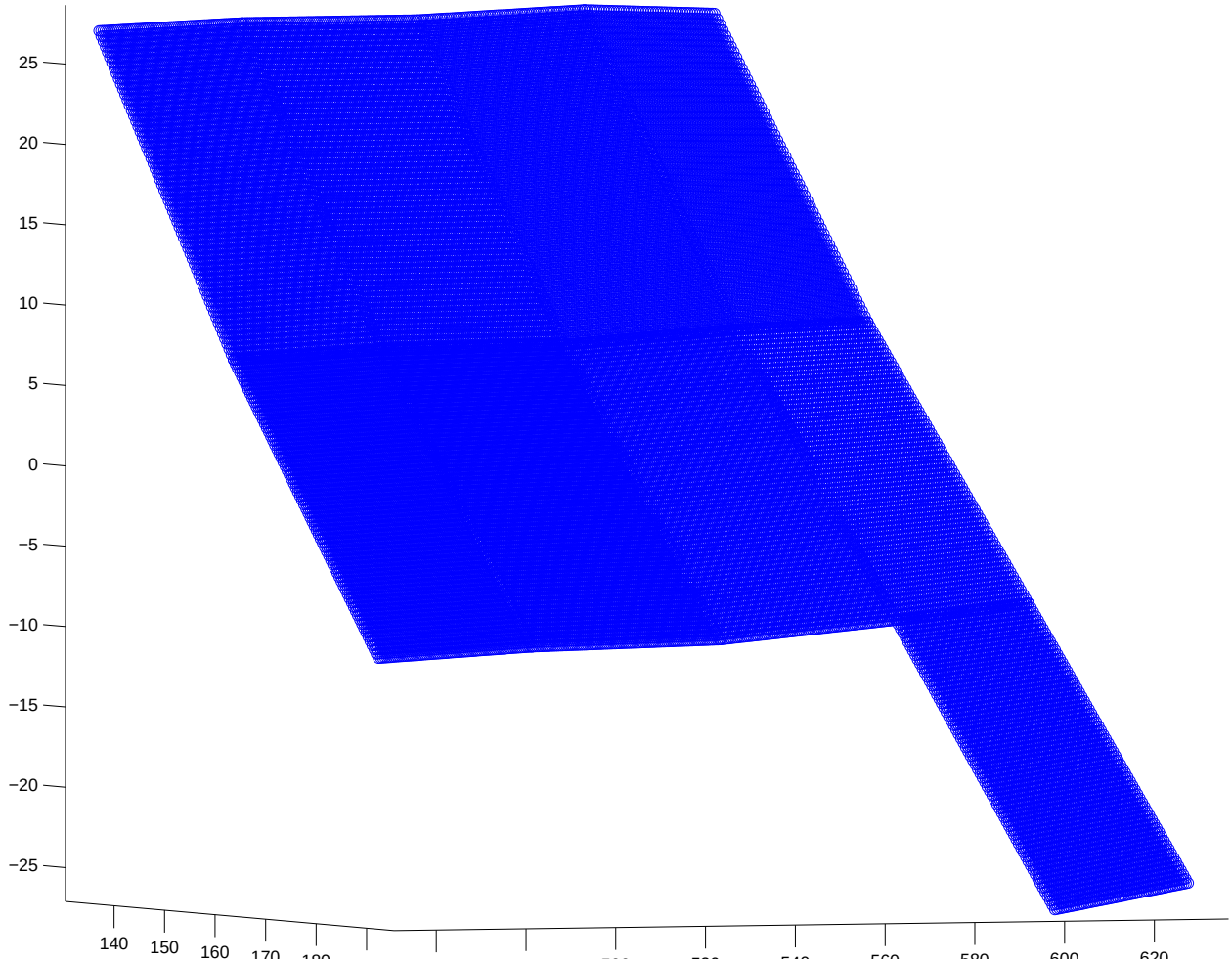

Figure 5.7: *xyz* plot of the geometry of the pictures. It can be seen that there are the same number of patches images squares.

Afterwards, it is possible to assembly all of the pictures and obtain a complete map of temperatures. In Fig. 5.8. the final measured geometry can be seen and after introducing this data in FLUENT it is possible to project to the outershell surface the temperatures and set the surface temperature as boundary conditions. In section *Experiment Results* the final temperature map can be seen.

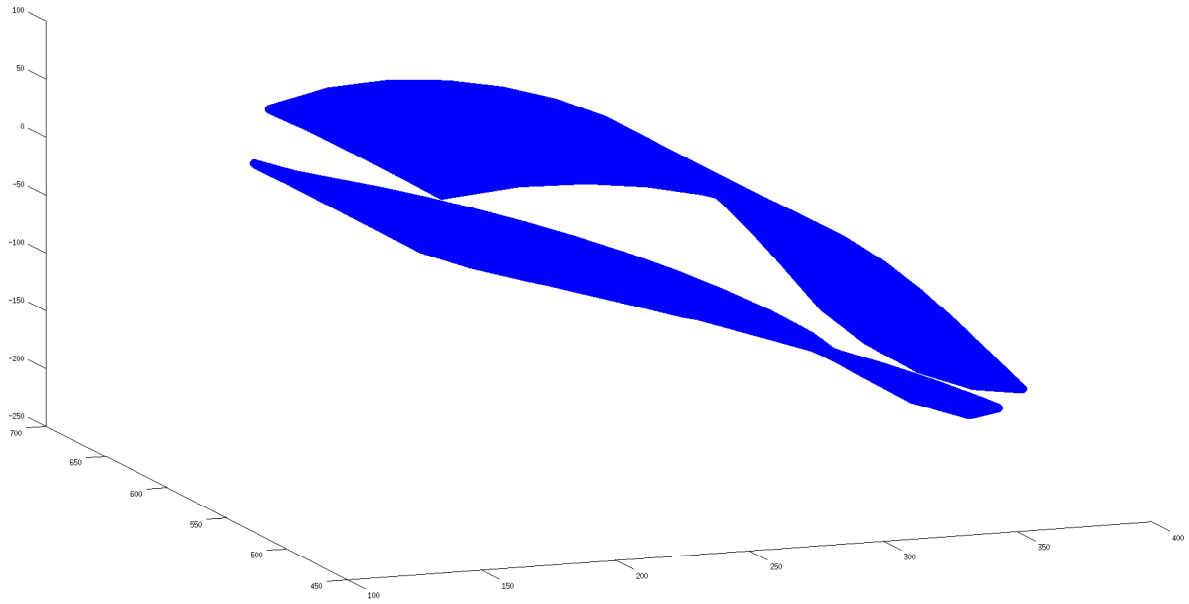

Figure 5.8: xyz plot of the geometry of the vane measure points. It can be seen that there are some spaces without information due to the lack of optical access.

5.3 Error of Measurement

Due to the fact that the camera has a precision of 0.01°, it is impossible to have an error lower than that value, although it is possible to have different additional sources of error. For example, if the window is opened for a very long time, the temperature of the vane can change. It was simulated with Matlab and the temperature change of 0.01 degrees was obtained during the first 100 ms, which is the time that it takes to take a picture. Another source of error could be the different angle that is used and the different position of the camera together with any unsteady conditions during the experiment. In order to check this situation, 2 pictures were taken which share the same square and they are compared to check the difference of temperature between them. It can be seen in Fig. 5.9 and 5.10 that this difference is very small.

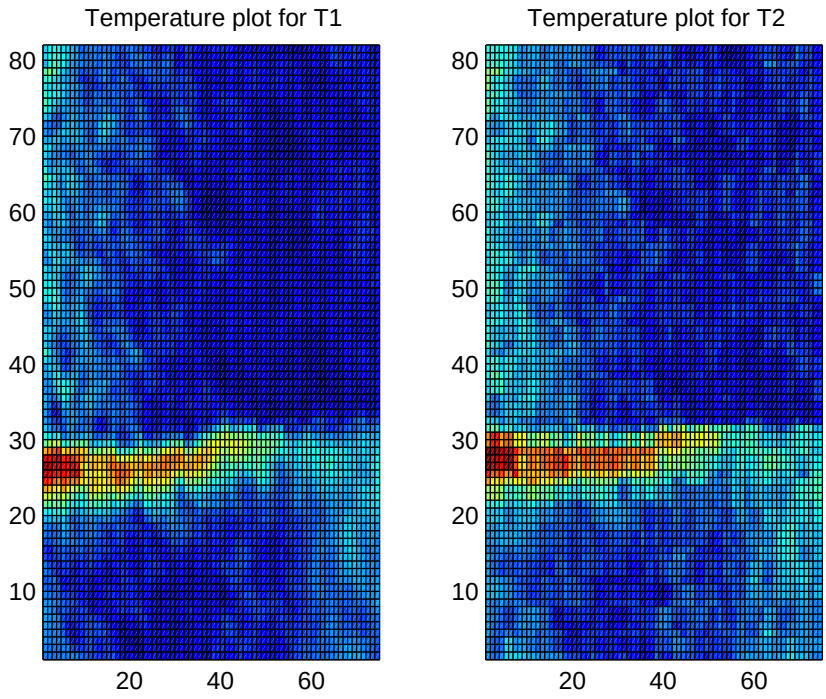

Figure 5.9: Comparison of the two pictures. It is important to take into account that originally they did not have the same number of pixels, but in order to compare them they are resized in order to be able to compare them.

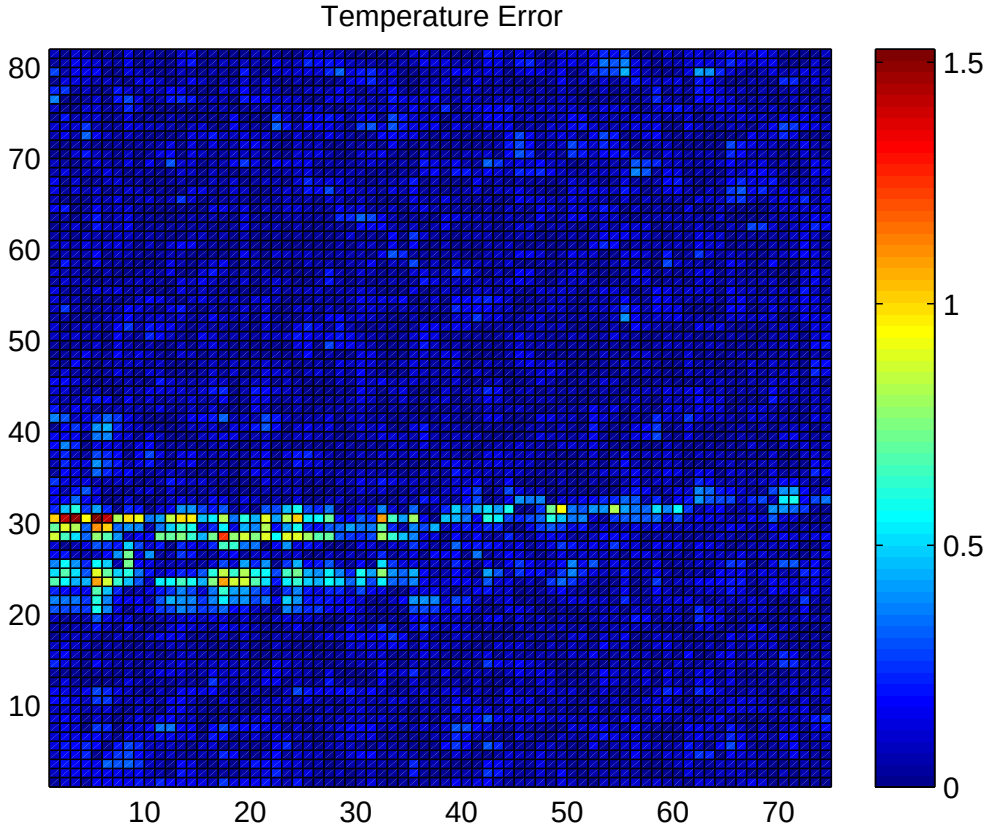

Figure 5.10: This figure represents the absolute temperature difference.

The average error is calculated using the mean of the temperature difference that can be seen Fig. 5.10. This error difference is 0.1022. This value is still very small for our experiment.

5.4 Experimental Results

Using the CFD software FLUENT it is possible to visualize all the data obtained from the experiment. First of all it is important to point out that the boundary conditions for these CFD simulations are the temperature measured with the IR-camera, the aluminium core as constant temperature (it is measured during the experiment and its value is 65℃), the air temperature is measured and its value is 28.5℃and all the physical properties of the materials for the simulation parameters. The experimental surface temperature map visualized in Fluent is shown in Fig. 5.11.

After checking that the data show a realistic map of temperatures, the next step is to calculate the heat flux and the convection heat transfer coefficient. In order to check that the 3D model calculates the convection heat transfer coefficient correctly, it is possible to validate it using Matlab and 1D heat transfer assumption. Knowing the map of temperatures and the temperature in the aluminium core and the temperature of the air, it is possible to perform these calculations. The difference between both models is 15%, so that the 3D simulation results. The resulting heat transfer coefficient distribution can be seen in Fig. 5.12. It is important to explain why there are some irregularities in the images. First of all, it is important to take into account that the shell of the vane was made with 5 different patches and some of them can be distinguished in the IR images. Another source of error is the extrapolation used by FLUENT in order to calculate temperature and convection heat transfer coefficient on the leading and trailing edges.

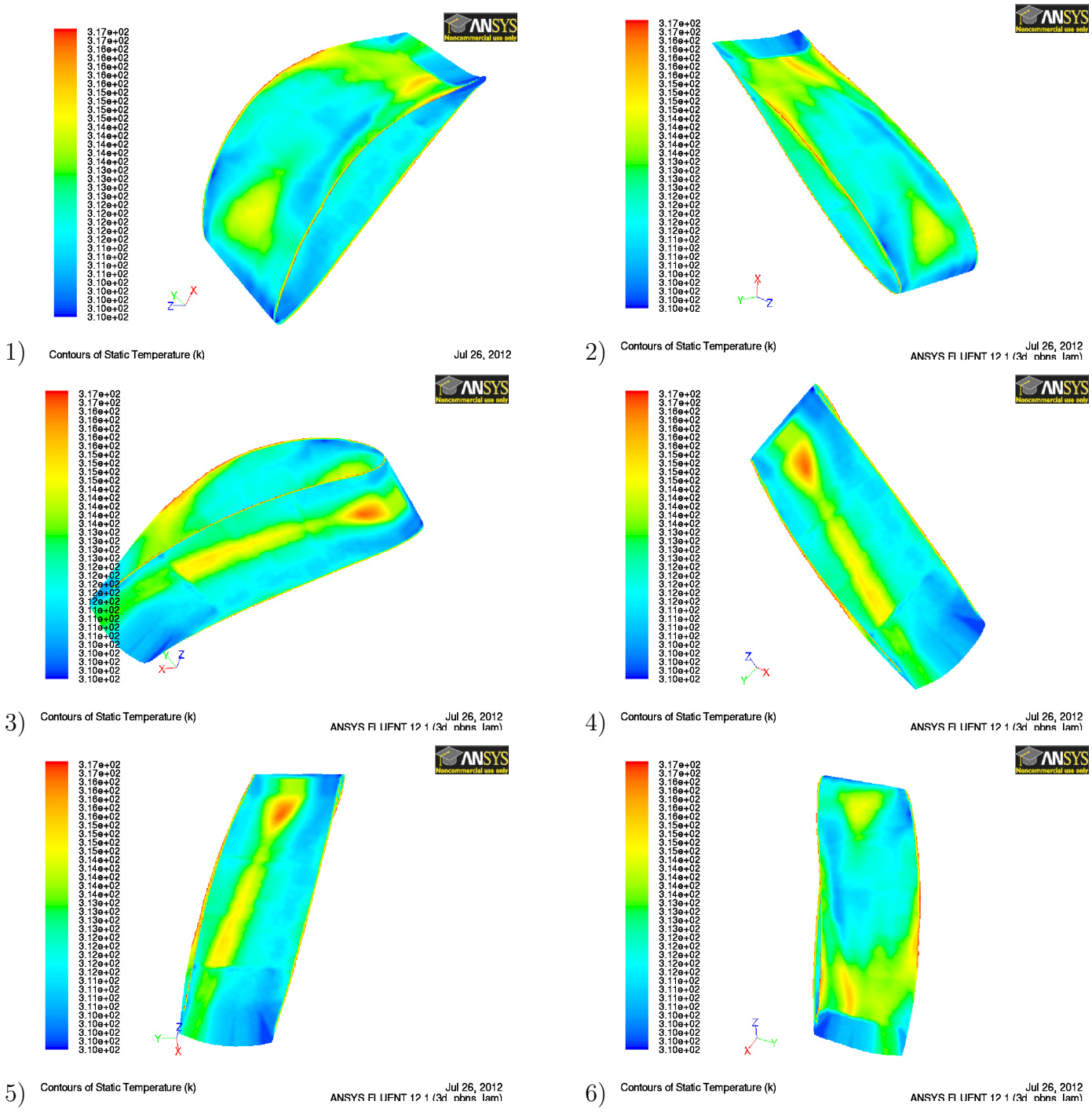

Figure 5.11: Experimentally measured vane surface temperature visualized in Fluent.

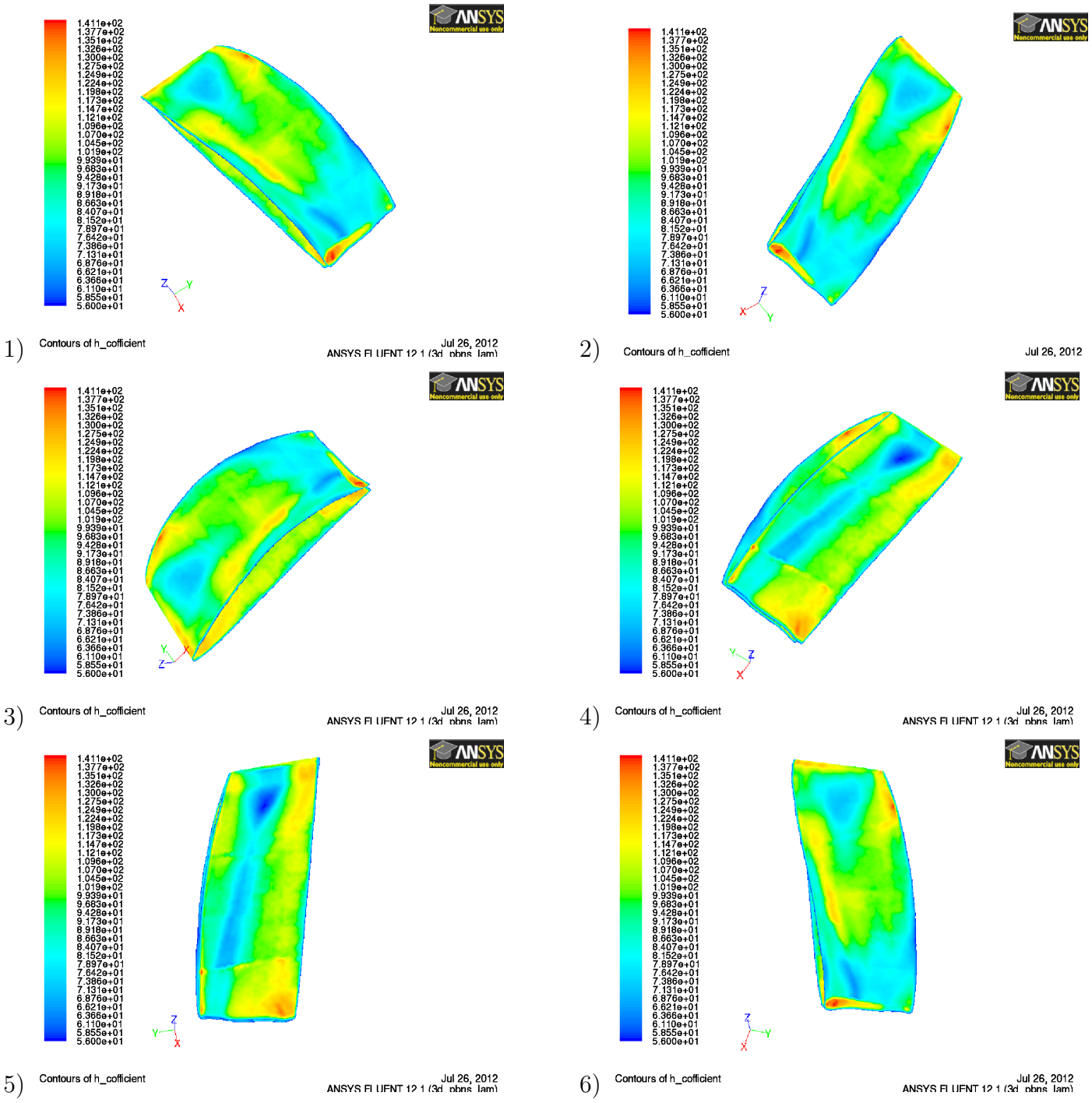

Figure 5.12: Calculated convection heat transfer coefficient map from experimental temperature distribution.

Chapter 6

Summary

6.1 Methodology

The methodology of the experiment is summarized in this section.

For heat transfer experiment first of all, it is needed to have a specially designed and instrumented vane. After all the problems with the detached shell from the first design after running the experiment, it was needed to manufacture our own vane shell using silicone instead of epoxy.

Then it is needed to paint the vane with the black coating. This black coating was applied using a spray gun.

Afterwards, the markers are made over the vane in order to know during the experiment which is the physical coordinates of the temperatures which are measured on the vane. In order to do these markers a traverse system is used and silver paint markers which have emissivity much lower than the emissivity of the black coating.

Later, the vane has to be mounted inside the rig. Once it is there, the vane is used for preparing the holes of the windows in order to have optical access for the IR-camera.

After this, the setup of the camera has to be done in order to calibrate the camera for the experimental conditions using external sources of temperature.

Then, the experiment has to be run and the IR-camera images have to be taken. During the experiment, 31 thermographs are taken with the IR-camera (17 for the pressure side and 14 for the suction side).

Finally, the post processing of the images is the last step. All the images are filtered and the useful areas from the pictures are selected. Afterwards, once all the images are assembled into a text data file, it is possible to export this data to FLUENT and run the simulation using this information.

6.2 Conclusions

The main conclusion from this project is that the CFD simulation from Volvo Aero does not fit totally with the experimental results that are presented in this paper. The suction side heat transfer distribution predicted relatively well with certain discrepancies but the pressure side heat transfer coefficient distribution is not predicted correctly as in experimentally obtained data of Fig. 5.12.

It can be seen in the Fig. 5.12 that the convection heat transfer coefficient is larger close to the shroud than to the hub. This could be due to the tip leakage flow.

Finally, another conclusion that should be taken into account is the difficulty to manufacture a vane composed of different materials. This can be a bottle neck for future experiments in this area using such a 3-dimensional vane design.

Bibliography

[1] C. Arroyo Osso, (2009) *"Aerothermal Inestigation of an Intermediate Duct"*, Thesis for the Degree of Doctor of Philosophy, Chalmers University of Technology

[2] Martin *Johansson*, Valery *Chernoray*, Linda *Strom*, Jonas *Larsson*, Hans *Abrahamsson "Experimental and Numerical Investigation of an Aerodynamically Loaded Guide Vane in a Turbine Duct"*, Proc. of ASME TURBO EXPO 2011, Paper no GT2011-46221

[3] T.*Povey*, K.S *Chana* and T.V *Jones "Heat transfer measurements on an intermediate-pressure nozzle guide vane tested in a rotating annular turbine facility, and the modifying effects of a non-uniform inlet temperature profile"*, Proc. Instn Mech. Engrs Vol. 217 Part A: J. Power and Energy

[4] Incropera, DeWitt, Bergman, Lavine (2007) *"Fundamentals of Heat and Mass Transfer"*, 6^{th} edition.

[5] J.P Holman, *"Heat Transfer"*, 10^{th} edition, McGraw Hill

[6] A.Kassab, E. Divo, J. Heidmann, E. Steinthorsson, F. Rodriguez, (2003) *"BEM/FVM conjugate heat transfer analysis of a three-dimensional film cooled turbin blades"*, International Journal of Numerical Methods for Heat and Fluid Flow, Vol. 13 lss: 5, pp.581 - 610

[7] Lars-Uno Axelsson, (2009) *"Experimental Investigation of the Flow Field in an Aggressive Intermediate Duct"*, Thesis for the Degree of Doctor of Philosophy, Chalmers University of Technology

[8] Johan Hjrne, (2003) *"Aerodynamic Investigation of Turbine Outlet Guide Vane Flows"*, Thesis for the Degree of Licentiate in Engineering, Chalmers University of Technology

[9] *Phoenix*^{TM} Camera System With RTIE. Version 120. Indigo Systems Corporation.